

## Acknowledgments

Oh! I have slipped the surly bonds of Earth  
And danced the skies on laughter-silvered wings;  
Sunward I've climbed, and joined the tumbling mirth  
Of sun-split clouds,  
and done a hundred things  
You have not dreamed of — wheeled and soared and swung  
High in the sunlit silence. Hov'ring there,  
I've chased the shouting wind along, and flung  
My eager craft through footless halls of air. . . .  
Up, up the long, delirious burning blue  
I've topped the wind-swept heights with easy grace  
Where never lark, or ever eagle flew —  
And, while with silent, lifting mind I've trod  
The high untrespassed sanctity of space,  
Put out my hand, and touched the face of God.

John Magee Jr.



Thank you for supporting me as I soar

The Copeland Fund  
Dr. Paul Kennard, NPS  
Laura Walkup, NPS  
Scott Beason, NPS  
Dr. Paul Edmiston  
Dr. Dan German

*Dedicated to Grandpa Bill. A wet bird never flies at night.*

## Table of Contents

### SUMMARY 4

### INTRODUCTION 5-25

*Glaciers 5*

*Storage Capacity 5-6*

*Flooding 7-8*

*Mechanisms of Jökulhlaups 8-13*

*Mount Rainier National Park 13-18*

*Current Research in Mount Rainier National Park 18-19*

*Hypothesis: Stagnation can be Predicted by the Chemical Composition of Water 19*

*Recent Research & Glacial Meltwater Chemistry 20-21*

*Focus on the Nisqually Glacier 21-24*

*Fe in the Ice/Meltwater 24-25*

### METHODS 26-28

*Sampling Approach and Locations 26*

*Field Methods 26-27*

*Inductively Coupled Plasma-Atomic Emission Spectroscopy 27-28*

### RESULTS & DISCUSSION 29-49

*Introduction 29*

*Sampling Locations 30*

*Physical and Chemical Measurements 31-37*

*Iron 37-40*

*Iron Speciation Analysis 40-42*

*Variables that Affect Fe Concentration 42-45*

*Temperature and Discharge Rate 45-46*

*Potential Origin of Free Metals in Glacial Meltwater 46-47*

*Anthropogenic Metal Sources and Notes on Sampling 47-48*

*Ecological Implications 48-49*

### REFERENCES 50-51

### APPENDICES

*Field Data 1 52-54*

*Bathophenanthroline Calibration Curve 2 53*

*ICP-AES Data 2 54-60*

Determining the status and level of glacial stagnation is important for protecting communities in areas downstream that would be affected by consequential outburst release floods. There are detectable chemical differences between glacial meltwater and mountain snowpack inlet streams that can be used to monitor glacial outflow. It is hypothesized that iron concentration, turbidity, temperature and pH levels may be used to monitor hydrology of the Nisqually Glacier in Mount Rainier National Park, Washington. A series of field tests (Fe, NO<sub>3</sub>, hardness, pH/conductivity/ORP/temperature, turbidity) provided preliminary data to compare with further analytical testing in the lab, including ICP-AES, a bathophenanthroline colorimetric test, and total organic carbon measurements. Analysis showed dissolved iron concentration to be statistically higher in glacial meltwater than in snowpack inlets ( $t=9.26$ ,  $p<0.001$ ). Fe levels decreased downstream, presumably due to dilution from snowpack inlet streams. Turbidity followed an equivalent trend, decreasing as the zero-turbidity snowpack melt diluted the river at increasing distances from the glacial terminus. Temperature measurements followed suit by increasing in value along the Nisqually River, presumably due to contributions from warmer snowmelt inlet streams. pH levels were detected at similar values for each of the sampling sites, but according to Anderson et al, a drastic change in pH would indicate a hydrogeological shift in the glacier. Thus, Fe, turbidity, temperature, and pH appear to be effective signals<sup>1</sup> for monitoring glacial output that may be quickly and easily tested using field kits. Utilization of a real-time method to test for stagnation would afford researchers the opportunity to predict jökulhlaups. Based on this work, it is also postulated that glacial meltwater may be an unappreciated source of nutrient Fe in river and ocean ecosystems. Future work includes continued measurements of Fe concentration, temperature, pH, and turbidity along with river flow to understand how these signals fluctuate as river flow changes. Daily measurements should be taken as close to the terminus as practical (i.e. Nisqually Glacier Bridge) to avoid increased dilution of glacial outflow signals. Continued measurements are important for chemical characterization of the Nisqually's glacial outflow. Correlating these results with ice velocity and/or ice elevation measurements would allot a geochemical profile of the Nisqually Glacier and River.

---

<sup>1</sup> A signal is defined as a solute that directly emanates from the glacier and could be used to monitor glacial output.

## Introduction

### *Glaciers*

Glaciers are actively moving, frozen rivers that store vast amounts of freshwater. Glacial ice forms when snow is consolidated by weight into condensed ice, free of air bubbles. Masses of ice can be defined as glaciers once they reach a sufficient size, in which their mass allows them to flow. Glaciers sculpt the surrounding landscape by grinding valleys in mountains via action between ice and rock moving against the bedrock. Many of the current glaciers formed during the last Ice Age 20,000 years ago by extensive accumulation of snow and lack of melting. Near 10% of the global land mass is covered by glaciers, which are found on each continent, although the vast majority resides in the polar climates. As an indication of scale, complete melting of the world's ice would result in an 80 m (262 ft) rise in sea level, covering major cities including Los Angeles, New York City, and Miami [1]. Glacial ice experiences melt due to high ambient temperatures, which is released from the glacial terminus into a melt river. Many of the world's rivers are glacially fed, including major rivers sourced from the Himalayas, the Andes, and similar landscapes (i.e. Indus, Ganges, Yellow, Yangtze rivers).

### *Storage Capacity*

Glaciers store water in daily, annual, and decade-long intervals depending on the structure of the individual glacier [2]. Glacial storage capacity and flow are dependent upon the glacier's characteristics (i.e. ice volume) and seasonal snow accumulation. More specifically, glacial storage has been observed to directly relate to mass input from precipitation and inversely relate to present ice volume [2]. The high storage capacity of glaciers and complex water flows

makes them important for hydrogeological studies. In addition to ice flow, glaciers transport liquid water within channels and conduits, creating a complex and variable hydrogeological system. Snow and other forms of precipitation settle on the surface of the glacier, either melting into surface water or saturating underlying firn [3]. During a melt season, surface water enters the englacial system through cracks and holes in the ice, and is transported deeper into the glacier via englacial pockets and conduits [2]. Eventually, these pathways feed into subglacial cavities, where all of the water flowing through the glacier mixes [2]. Debris collected from the ice grinding against the bedrock is transported with the water out of the terminus (end of the glacier); the mixture of water and debris is known as glacial outflow (Figure 1).

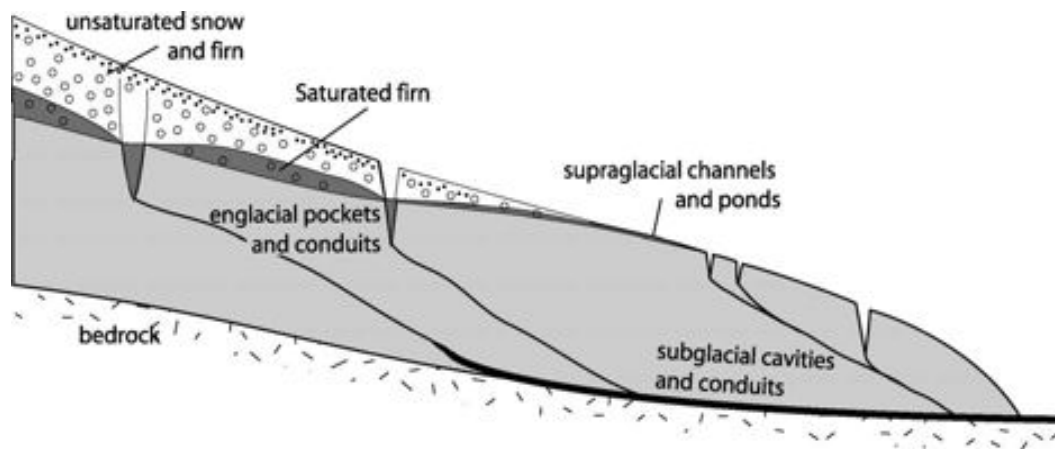


**Figure 1** [2]. The Glacial Hydrological System: Surface water enters englacial pockets and conduits. This water travels to subglacial cavities and conduits, where the subglacial and englacial water mix together with underlying debris. The water/debris (outflow) releases through the glacial terminus.

Precipitation (i.e. rainfall) enters the glacier's hydrogeological system and contributes to the glacially-produced meltwater. The amount of flow and melt depends on how much precipitation has recently fallen and air temperature [4].

## *Flooding*

Erratic flow dynamics in glacial hydrogeological system can lead to hazardous flooding events. Glacial flooding is significant for a large percentage of our population. All glaciers are prone to high water volume release, regardless of type or location. Flooding occurs through periodic or occasional releases of large volumes of liquid water sequestered within cavities of the glacier [4]. Glacial release, or outburst, floods are powerful enough to destroy buildings and infrastructure lying in the flood path, and drastically change river channel paths [4]. It is difficult to predict the time and magnitude of release floods due to complex and changeable internal glacial structures [4].

The term given to a release flood is a jökulhlaup, which is an Icelandic word that is generally described as a catastrophic outburst event. Jökulhlaups are relatively frequent in Iceland, which, by landmass, is covered by 10.9% of glacial ice [5]. Some jökulhlaups are extremely catastrophic outburst flood events. A number of the most destructive jökulhlaups have been recorded in volcanically active regions where the underlying bedrock melts a significant portion of the glacier [4]. The higher degree of damage is primarily attributed to debris flow characteristic of volcanic geology that enhances the power of the violently flowing water [4]. Intensity of these jökulhlaups decreases as volcanic and geothermal activity decreases, and vice versa [4]. On rare occasion, jökulhlaups may occur without substantial water storage, as glacial ice may melt very quickly with increased volcanic heating [6].

The occurrence of jökulhlaups may be indicative of glaciological changes due to measurable glacial snout<sup>2</sup> oscillations [4]. These oscillations occur seasonally with surges and climate changes, causing the terminus to advance or recede [7]. Surges are quasi-periodic

---

<sup>2</sup> Glacial snout is another term for glacial terminus

accelerations in glacial ice in response to the climate and the hydrogeological mechanism of the glacier [7]. In cycles of retreat, outflow<sup>3</sup> may pool subglacially and release as the ice retreats away from the subglacially pooled water, deconstructing the water barricade [4].

When feasible, the magnitude of a release flood may be forecasted using an equation calculated by Clague and Mathews (1973) [4]:

$$Q_{\max} = 75\left(\frac{V_o}{10^6}\right)^{0.67}$$

This equation (Equation 1) can be used to estimate the water volume released from ice-dammed lakes<sup>4</sup> in the glacier ( $V_o$ , m<sup>3</sup>) to the peak flood discharge ( $Q_{\max}$ , m<sup>3</sup>s<sup>-1</sup>) [4]. The constants in the equation have been modified by researchers through the years, as this formula is empirically based [4]. One researcher described the equation as “confound(ing) understanding but seems to give reasonable results” [4].

### *Mechanisms of jökulhlaups*

Mechanisms for jökulhlaups are poorly understood. Understanding the causes for glacial water storage and measuring meltwater flows of jökulhlaups is essential for predicting events to warn people in the floodplain and develop effective mitigation strategies for communities downstream [6]. Learning the englacial and subglacial channeling systems in various geological conditions may afford useful information for areas currently experiencing jökulhlaups,

---

<sup>3</sup> Outflow describes the composition and rate of material flow that releases from the glacial terminus.

<sup>4</sup> Ice-dammed lakes develop when a pool, or lake, of meltwater forms englacially or subglacially. The lake water is held in place by ice barricades that seal off cracks where the water could re-enter the actively flowing system [4].

potentially offering a base for predicting the magnitude and relative time of future events. More importantly, measuring glacial meltwater output with time is necessary when attempting to predict flooding events. It is known that jökulhlaups typically occur during the summertime when peak melting and drainage network development occur, but events have been recorded to take place in the winter as well [4]. It has also been observed that expanding glaciers generate less meltwater than dwindling glaciers [2]. This stored water may accumulate though water stored in firn, englacial pockets, and subglacial cavities/conduits before releasing via a jökulhlaup (Figure 1). Stored meltwater may pool into subglacial lakes by ice/rock barricades that act as dams. The ice/rock barricade that contains the meltwater in a subglacial lake determines the mechanism of release; different ice and rock barricades breach and release water in different ways [4]. The three most common features include moraine-dammed lakes, ice-dammed lakes, and subglacial lakes. Ice dams that contain the meltwater lakes will ultimately fail due to rupture of the barricade, typically in response to the amount of water or glacial movement [8]. Thick glacial ice is an effective dam to subglacial lakes, as the ice seals off cracks where the water may escape [6]. On the contrary, thin ice residing over a deep lake is an ineffective dam, as the water is denser and more abundant than the ice, and may lift the weak glacial dam off to release (Figure 2) [6].

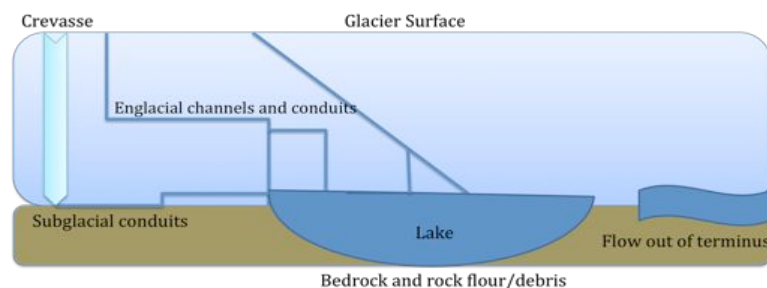


**Figure 2.** Cross-section of a Subglacial Lake: This is a typical subglacial lake, where water is fed into the lake cavity through multiple pathways. Crevasses, or cracks in the ice, may transfer surface water to the subglacial conduits. Englacial channels transport water into the lake or subglacial conduits. The lake is secured by overlaying ice that acts as a dam, containing the meltwater. A subglacial lake may burrow into underlying bedrock and debris.

Predicting floods is difficult due to the complexity of meltwater flow through the glacier. Meltwater is known to enter and exit the glacier through channels at the glacier bed (Figure 1) [4]. Alterations in the glacier's hydrological system may cause pressure changes in the barricaded area, which may trigger meltwater release to relieve the pressure. Water release enlarges the subglacial drainage pathways via mechanical and thermal energy when the water moves through the pathways. The water gains speed and volume while traveling through the drainage pathways engraved in the ice, elevating the temperature of the flowing water, melting the ice, and enlarging the drainage pathway. Larger drainage pathways allow more water and debris to flow, creating catastrophic conditions for locations downstream. The outburst flood will cease once the meltwater lake has emptied, or ice creep<sup>5</sup> from drastic changes in pressure between the water-filled and emptied pathways blocks the pathway. This phenomenon is visible in jökulhlaup hydrographs by a leveling of discharge rate over time [4]. The Grímsvötn Lake in Iceland is one of the most studied subglacial lakes. The Grímsvötn resides over a geothermally active volcanic landscape, which has caused overlaying glaciers to melt into the lake, producing large jökulhlaups in 1934, 1938, and 1996 [9]. This ice-dammed lake is covered by 300 m of ice on the Vatnajökull glacier, and is visible by a 10 m depression directly above the lake on the glacier's surface [10].

The Grímsvötn has a versatile event history. Jökulhlaups from this subglacial lake have occurred with and without local volcanic activity [10]. Over the past few centuries, events in time with eruptions have been documented on the order of one per decade, while those unrelated to eruptions have occurred within the span of 1-9 years [10]. These more periodic jökulhlaups

---

<sup>5</sup> Ice creep occurs when ice moves slowly or deforms under the influence of stress (i.e. pressure).

may not be predicted using Equation 1 due to the unsystematic nature of geothermal activity, but may be forecasted using other predictive signals. A hydrograph of recorded jökulhlaups from the Grímsvötn (Figure 3) shows the overwhelming flood volume released in the 1934, 1938, and 1996 events that were initiated by volcanic eruptions. Casualties and infrastructure destruction resulted from these events, resulting in concern by communities that reside in the flood path of a glacially capped, active volcano.

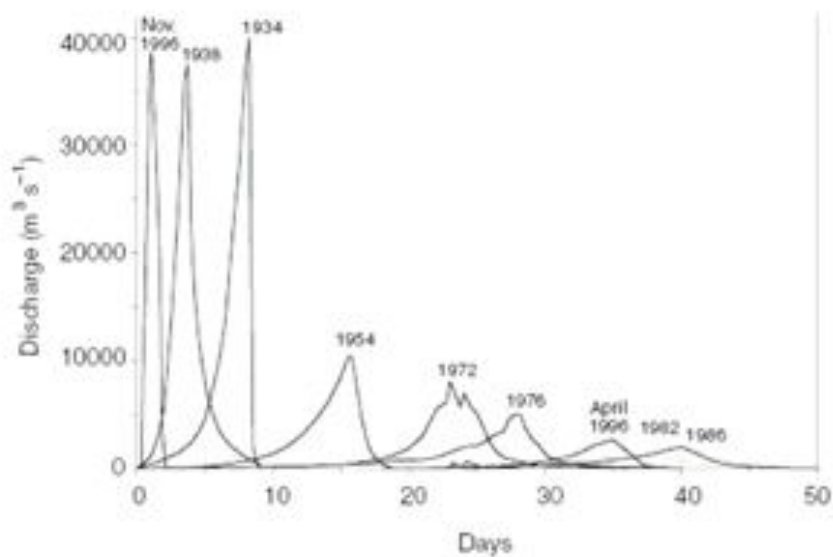


**Figure 3** [10]. Jökulhlaup hydrograph from Grímsvötn, Iceland. Events in 1996, 1938, and 1934 were in time with volcanic eruptions, while the remaining events were not in time with eruptions. Note the April 1996 event between Days 30-40: this is not related to the November 1996 event.

Peak flows for the 1930's events were 25,000 - 30,000 m<sup>3</sup>/s with 4.5 km<sup>3</sup> of total discharge volume in 1934 and a slightly lower volume in 1938 [10]. This flow rate could fill 76 Olympic size pools (500,000 gallons) every second. A record setting 40,000 – 50,000 m<sup>3</sup>/s peak flow occurred in the 1996 jökulhlaup, which released 3.6 km<sup>3</sup> of discharge [10]. The Grímsvötn epitomizes a non-systematic, repeated outburst event system because it resides over a geothermally active zone [2]. Generally, glaciers that reside over geothermally active areas exhibit non-systematic (i.e. unpredictable) behavior due to unforeseen fluctuations in thermal

activity. Glaciers that do not reside over volcanic landscapes are more predictable as outburst events correlate with weather and advance/retreat of the glacier. Therefore, volcanic glaciers may not be compared with non-volcanic glaciers with regard to outburst events. Fluctuations in geothermal activity caused the overlaying Vatnajökull Glacier to melt and feed in meltwater to the Grímsvötn glacial channel at an unpredictable rate [2]. The filling of the Grímsvötn is visible in the elevation rise and drop of the subglacial lake, which is monitored by a navigational GPS in the center of the ice shelf that resides over the lake [9]. Researchers have noted that the lake fills, and rises in elevation, with increased geothermal activity. This activity melts surrounding ice and snow into the lake. Figure 4 illustrates the change in elevation of the subglacial lake in contingency with pressure data from 2003-2004. A significant drop in pressure indicates the lake has emptied, which may trigger a subglacial eruption from the volcano residing beneath [9].

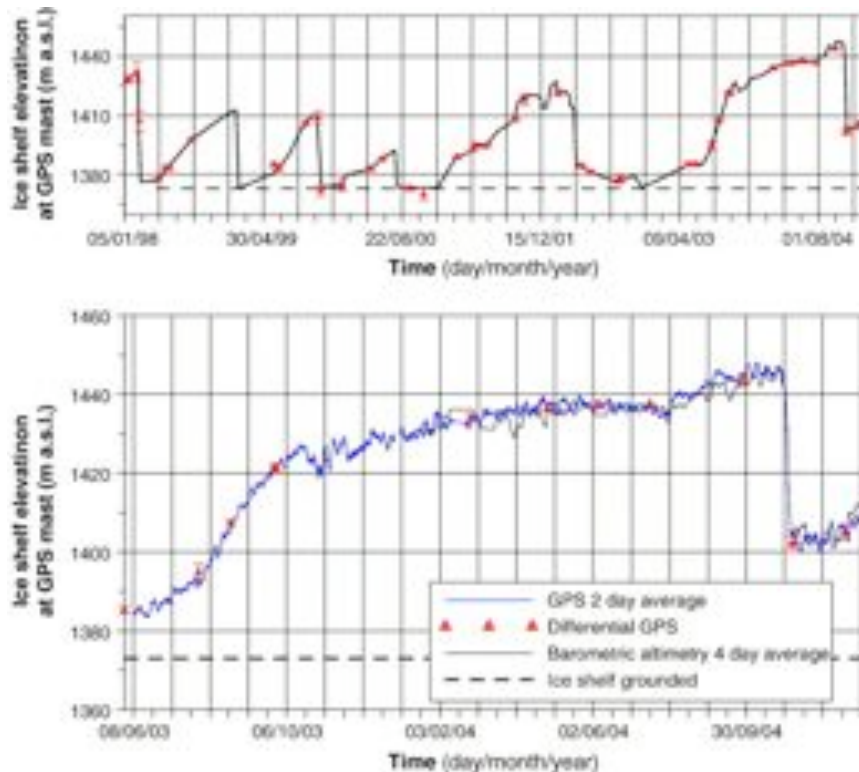


**Figure 4** [10]. Elevation and Pressure Changes Associated with the Grímsvötn Lake: Top: elevation changes in the above ice sheet indicate the lake is filling with water (rise) or emptying (fall). Bottom: the pressure inside the lake cavity slowly rises as the lake continues to fill with water, and drastically decreases as the lake empties.

The Grímsvötn is under continued observation, and researchers utilize the elevation and pressure data to predict when the next jökulhlaup will occur.

### *Mount Rainier National Park*

Mount Rainier National Park in Washington State is a glaciated volcano with a substantial history of glacial flooding events. Mount Rainier National Park houses a total of twenty glaciers, with six major glaciers capping the volcano oriented in a star-like pattern. The park's six major glaciers are the Tahoma, Carbon, Winthrop, Ingraham, Emmons, and Nisqually (Figure 5).

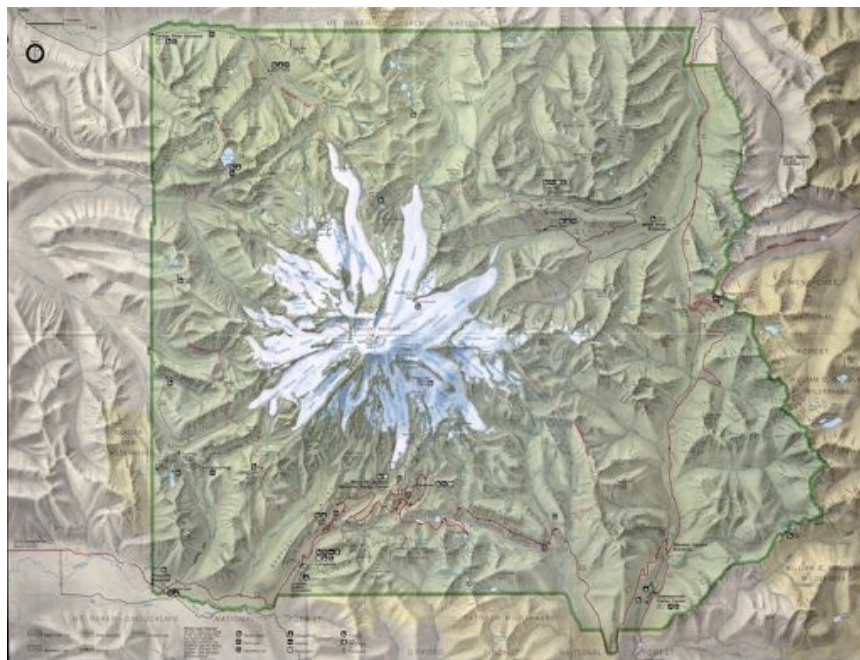


**Figure 5.** Topographical Map of Mount Rainier National Park. This view focuses in on the glaciated area of the park, visualizing the glaciers that are situated around the volcano. Map from [www.mora.gov](http://www.mora.gov).

In total, Rainier is covered by the largest network of glaciers in the contiguous 48 states [8]. The glaciers have areas decreased 22% (25% by volume) over the past ten years due to melting from rising temperatures. The newly exposed soil underneath becomes vulnerable to entering the

streambed with glacial outflow and rainfall [8]. Heavy volumes of water from rainfall and the release of pooled glacial melt can carry this soil downstream in a general debris flow or jökulhlaup, which places downstream human activities at risk.

Examples of potential damage that could result from a large jökulhlaup in the park may be drawn from recent events on the southwest face of the volcano. The South Tahoma Glacier is situated between the Tahoma and Nisqually glaciers, and is recognized for producing periodic jökulhlaups (Figure 5). The South Tahoma Glacier released fifteen recorded jökulhlaups between 1986 and 1992 [11]. Combined with debris flows and landslides, the outburst floods transported significant loads of sediment during these events. Witnesses associated these events with extremely loud noises, strong winds, dense clouds of dust, and significant ground shaking. The Nisqually Glacier has also experienced significant debris flows triggered by jökulhlaups. Events in 1926, 1932, 1934, and 1955 destroyed both roads and bridges that pass over the Nisqually River [11]. The Nisqually underwent a period of recession from 1850-1963 with a slim window of advancing in the early 1900's [12]. A relatively short era of stagnation was recorded in 1951 when the terminus appeared to be a mass of debris-covered ice. This period directly overlapped with a kinematic wave that propagated down the glacier, overtaking the stagnant ice and sending the Nisqually into a period of advance [12]. Additionally, the 1950's produced catastrophic outburst release floods that were directly attributed to stagnant ice pooling and releasing glacial outflow (jökulhlaup) [13]. Currently, the Nisqually is losing ice at a rate over six times the historic average ice loss. In Summer 2011, a preliminary field project concluded that more than half of the lower Nisqually glacier was becoming stagnant. This stagnant ice has the potential to behave similarly to the 1950's Nisqually, hosting catastrophic outburst flood events that could potentially destroy infrastructure downstream. The Park's main

road, work and visitor centers lie in the direct path of a jökulhlaup, leaving the area in a high-risk zone. Since the 1955 and 2006 events, the Nisqually River has continued to fill with sediment, which has decreased the river's capacity to transport material and will result in further flooding. Several other glaciers in the park have been expressing stagnation characteristics as well [13].

The Nisqually recently experienced an outburst flood on October 27 of 2012, attributed to heavy rainfall pooling in the terminus, and releasing (Figure 6).

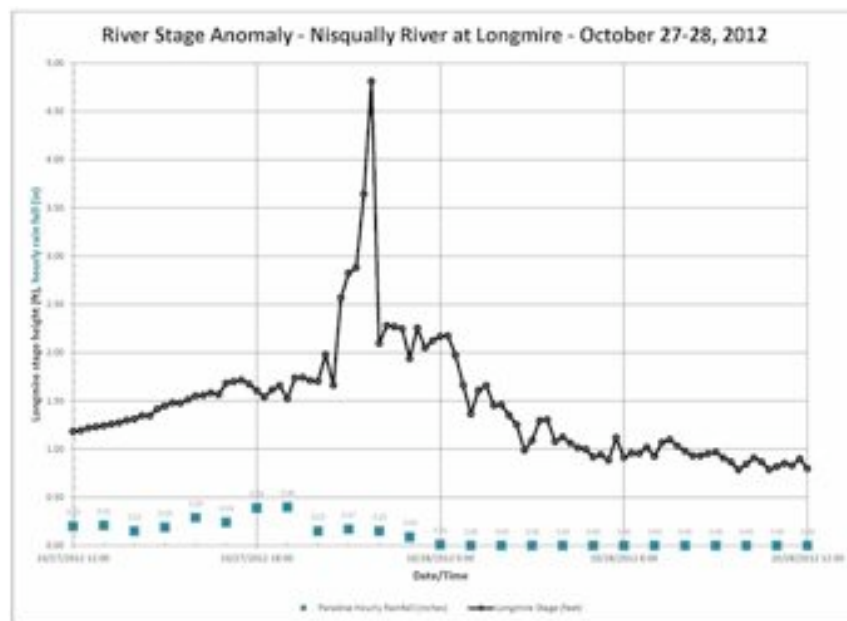


**Figure 6:** Hydrograph of the October 27-28, 2012 Outburst Event on the Nisqually River at Longmire. Stage height is represented by the black points and line, while the hourly rainfall is represented by the blue squares. Graph attained from [www.mora.gov](http://www.mora.gov), produced by Scott Beason.

The sharp peak in stage height, which is proportional to flow rate, indicates the jökulhlaup floodwater passing through Longmire. This spike shortly follows the peak in hourly rainfall, visible through the time lag between peak rainfall and peak stage height. This lag indicates the time between water build-up in the terminus, and release as the barricade was broken.

Additional, less destructive events occurred in the late 1960's through the mid 1980's [11].

Photographs of the 1934 and 1955 jökulhlaups, and consequential aggregation from the jökulhlaups were recorded and are listed below (Figure 7).



**Figure 7a.** Photographic Record of the Nisqually River: Top left: Nisqually River prior to the 1934 jökulhlaup. Top right: Aggregation aftermath of the 1934 jökulhlaup, photo taken in 1947. Bottom left: aggregation aftermath of the 1955 jökulhlaup, photo taken in 1965. Glacier Bridge can be clearly seen at the vertex of the river bend in the middle of the photo.



**Figure 7b.** Historic Photos of the Nisqually's 1955 jökulhlaup. From left to right: Damage on the park's main roadway at Mile Marker 6; Longmire flooding; photo from an occurring outburst flood in 1939. Photos attained from Archives in Longmire Library, Mount Rainier National Park.

The 1934 and 1995 jökulhlaups both destroyed the concrete bridge that connected the park's main roadway over the Nisqually River (visible in Figure 7a). Heavy rainfall in 1934 caused a

massive buildup of water in the glacial terminus, leading to the jökulhlaup. In 1955, a significant amount of stagnant ice had developed, which led to englacial and subglacial pooling of meltwater, resulting in a catastrophic jökulhlaup [11]. Understanding how these stagnation events can be identified is of great interest.

### *Current Research in Mount Rainier National Park*

Due to the location and high number of visitors, extensive research is conducted in Mount Rainier National Park. Studying floods is particularly important because there is infrastructure at risk of damage. Several studies have been conducted on the Nisqually Glacier by National Park Service researchers and graduate students from regional universities. In the past five years, ice velocity and rock displacement techniques have been used to determine the stagnation status of a glacier. In the summer of 2011, the Mount Rainier park geologists concluded that more than half of the lower Nisqually Glacier was stagnating as a result of extremely slow and zero valued ice velocities [14]. Such a large portion of stagnant ice has not been seen since the 1950's, when multiple jökulhlaups destroyed significant infrastructure in the flood path [14]. Determining the level of glacial stagnation is useful because stagnant ice is directly related to jökulhlaups. Stagnant ice can interrupt the contingency of englacial and subglacial drainage pathways. Blocked drainage pathways pool meltwater, creating meltwater lakes that are highly prone to release via a jökulhlaup. A method to confidently detect stagnation and consequential catastrophic outburst events has yet to be determined.

An alternative approach to stagnation detection is to examine the composition of the meltwater to discern if there are chemical indications of stagnation. Though a chemical analysis of glacial meltwater has not yet been conducted to determine stagnation, basic hydrological

studies have identified a number of chemical species that are present and measureable in glacial meltwater. Once determined, monitoring studies could be developed to detect normal and abnormal levels of these chemical signals. Chemically based mixing models have previously been developed for glacial drainage systems to surmise subglacial and englacial solute compositions. Subglacial water is thought to contain high solute content from direct contact with finely ground rock particles from the bedrock, while englacial water is assumed to have little contact with solutes from debris-lacking ice [4]. Glacial outflow is modeled to contain a solution of englacial and subglacial water, resulting in mixed composition. Results from composition studies are useful baseline data for this alternative approach, and provide values to compare with newly collected data, however, new approaches are needed to detect stagnation.

*Hypothesis: Stagnation can be Predicted by the Chemical Composition of River Water*

In Mount Rainier National Park, it is predicted that stagnant/dead ice melt below the active South Tahoma Glacier will cause further debris flows as stored sediment in the melting ice releases into the streambed [11]. Though the exact time of each jökulhlaup has not been confidently predicted, a common trend has been observed where releases occur during uncharacteristically warm or heavy rainfall autumn days. A similar trend is predicted for the Nisqually Glacier, where stagnant ice may be pooling meltwater englacially and/or subglacially, putting the glacier at a high risk of releasing a catastrophic jökulhlaup [11]. Herein, it is hypothesized that stagnant ice may be detected by chemical signals present in the meltwater. More specifically, glacial meltwater flow may be confidently measured using the following signals: metal ion concentrations, salt concentrations, total organic carbon (TOC), and turbidity.

## Recent Research & Glacial Meltwater Chemistry

When assessing the foundation for testing the hypothesis of glacial stagnation, melt water chemistry may be useful to consider if it is useful to examine other geochemical studies. Reports of stagnant ice have been documented around the globe, with a number of the most famous studies in Antarctica, Iceland, the Cascades, and Alaska. Many studies have been conducted at various locations to monitor glacial outflow, and to measure the concentration flux of chemical species over a given time. A select number of these studies are described in Table 1, which provides an overview of the major chemical species measured in these glacial outflow studies. These studies were conducted to collect baseline data on the chemical species present in glacial meltwater, not with the intention of measuring stagnation.

**Table 1:** Overview of Glacial Outflow Studies.

Study	Species Measured	Reasoning Behind Measurements
Anderson et al.	K Ca Mg Na Si Cl SO <sub>4</sub> HCO <sub>3</sub> pH	To understand signature baseline solute concentrations, oscillations in discharge, and electrical conductivity during the summer on the Kennicott Glacier [15]
Marx et al.	Li Be Sc Ti V Cr Co Ni Cu Zn Ga Rb Sr Y Zr Nb Cd Sb Cs Ba La Ce Pr Nd Sm Eu Tb Gd Dy Ho Er Tm Yb Lu Hf Ta W Pb Th U	To understand the overabundances of certain elements seen on the surface of alpine glaciers in New Zealand (speculated to arise from Australian dusts) [16]
Larson et al.	Ca Mg K Na SiO <sub>2</sub> HCO <sub>3</sub> SO <sub>4</sub> Cl	To compare and contrast chemical compositions of two rivers with similar vegetation but different local geology. Also, to determine what extent geochemical reactions influence the chemical composition of meltwater [17]
Lapo, Kristiana	H <sub>2</sub> CO <sub>3</sub> HCO <sub>3</sub> CO <sub>3</sub> SO <sub>4</sub> Cl F NO <sub>3</sub> Major ions	Currently being complete to use glacial meltwater chemistry to evaluate hazard potentials for Rainier, and characterize seasonal and geographic changes visible in meltwater chemistry [24]

Each of the review papers described in Table 1 have shown both significant and insignificant concentrations of the measured chemical species. The study by Anderson et al showed measurable concentrations of the species K, Ca, Mg, Na, Si, Cl, SO<sub>4</sub>, HCO<sub>3</sub>, and pH, and

concluded that the hydrogeochemistry of rivers directly reflects upon changing conditions in subglacial hydrogeological mechanisms [15]. Despite the previous studies, a number of important chemical signals including dissolved transition metals and turbidity have not been examined.

### *Focus on the Nisqually Glacier*

A logistical challenge for researchers has been safe and efficient travel to sampling locations at the glacier or river under study. Due to the proximity of Mount Rainier National Park, the Nisqually Glacier and River have proven easy to access and have baseline data covering many years. The Nisqually Glacier is one of the focal points for monitoring and predicting outburst floods in the United States. Understanding the Nisqually Glacier's behavior has been a focus for the Park Service and for this research project.

Current studies on the Nisqually Glacier are being conducted by park and regional geologists to detect the level of stagnation on the lower Nisqually; stagnant ice on the Nisqually could potentially produce jökulhlaups, much like those predicted for the South Tahoma Glacier. Researchers have previously examined the composition of the Nisqually's glacial outflow to see what chemical species are present in the meltwater (not to measure stagnation) by measuring soluble analyte concentrations including  $\text{SO}_4^{2-}$ ,  $\text{NO}_3^-$ ,  $\text{Cl}^-$ ,  $\text{PO}_4^{3-}$ , alkali elements, etc., but have yet to monitor  $\text{Fe}^{2+}/\text{Fe}^{3+}$  ion concentrations. These analytes were found by Mount Rainier park geologists to have the following concentrations (Table 2):

**Table 2:** Soluble Analyte Concentrations of Measured Species in the Nisqually River. Data from the geology department archives at Mount Rainier National Park. Data point and location 407: Nisqually River at Longmire, 10 July 2002 at 8:00AM. One value for each (not averages), selected to match with dates/times of sampling for this project.

Soluble Analyte	Concentration (ppm)
SO <sub>4</sub> <sup>2-</sup>	0.58
NO <sub>3</sub> <sup>-</sup>	0.021
Cl <sup>-</sup>	6.38
PO <sub>4</sub> <sup>3-</sup>	0.024

Much like the previous studies on meltwater composition listed in Table 1, the soluble analytes measured in Table 2 represent baseline data of a few measurable species that exist in the meltwater. But with the new approach of measuring glacial stagnation via chemical signals, it is desired to measure a larger suite of species. The goal for this project is to develop a method to test for glacial stagnation using chemical signals and real-time measurements with field kits and chemical sensors. Utilization of a real-time method to test for stagnation would afford researchers the opportunity to predict jökulhlaups, and potentially spare communities downstream of preventable damage and casualty. Ideally, outflow would be measured volumetrically at the glacial terminus, but this task is difficult and dangerous due to imminent hazards (i.e. rock fall and difficult terrain). Outflow signals would be ideally monitored at distances downstream from the terminus, but dilutions from snowpack melt tributaries contaminate chemical signals of glacial outflow. The research herein will anticipate whether

daily temperature cycle, total dissolved solids (TDS), and/or conductivity measurements can be used to correct for meltwater dilution from these snowpack melt tributaries. Flow rate of the outflow is hypothesized to be proportional to metal ion concentrations, and more specifically Fe concentration. Multiple full-metal surveys of water collected along the Nisqually River were conducted to find concentration values of Fe. Samples were collected as close to the terminus as practical, and at various distances downstream to determine how the detected signals diluted further from the terminus (Figure 8). Snowpack melt tributary streams directly feeding into the Nisqually River were also measured to study their chemistry and impact on chemical signatures from the glacier so that a mechanism by glacial output could be quantified by chemical analysis of water at downstream sampling locations.

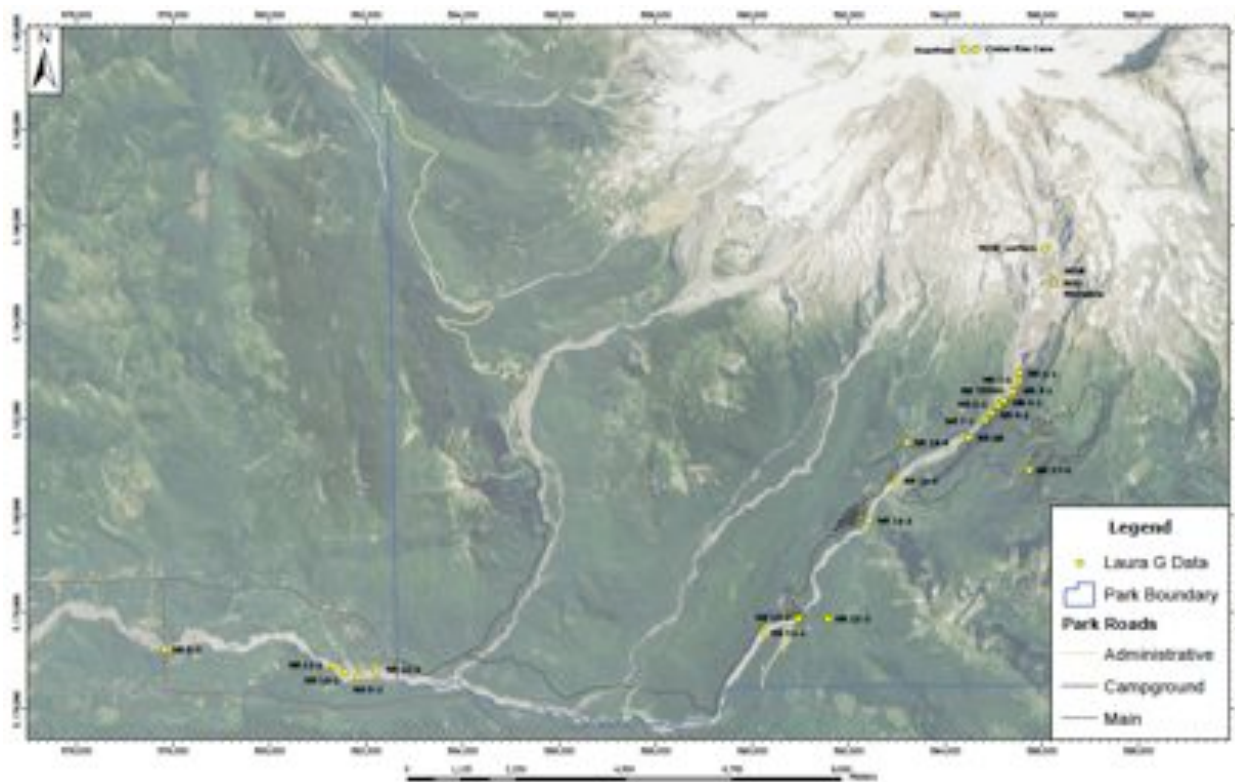


**Figure 8:** Topographical Map of the Southwest Face of Mount Rainier. Each yellow dot indicates a sampling site, characterized by an associated site name. GPS coordinates were calculated on the UTM-NAD83 coordinate system. Map created with Arc GIS.

Water samples and field readings were collected during various times of day to measure signal fluctuation throughout a daily cycle. Soluble Fe concentrations were measured in ice, snow, and meltwater samples to understand the transformation of Fe between the deposited snow, consolidation into ice crystals, and meltwater.

### *Fe in the Ice/Meltwater*

The measurement of dissolved Fe in glacier meltwater is a novel approach that may seem counterintuitive. Soluble Fe is not normally found in water due to the reaction with  $O_2$  to form  $Fe_2O_3$ . However, recently a team of Korean researchers observed that photochemical reactions involving Fe occur in what is known as the ice-grain boundary (Figure 9). This boundary is a vein-like network of liquid that travels in between the solid, crystalline ice [18]. The crystalline ice complexes push foreign items out of ice into a surrounding border on the surface (ice-grain boundary) where photochemical reactions occur [18]. More specifically, iron oxides undergo photoreductive dissolution in the boundary, which deconstructs  $Fe_2O_3$  into soluble Fe species of  $Fe^{2+}$  or  $Fe^{3+}$ . Species are highly prone to photochemical reactions in the ice-grain boundary because of the high concentration of protons (i.e. low pH) and exposure to UV light over the course of years. Kim et al observed that oxalic acid forms strong surface complexes with iron oxide in the boundary, leading to the highest photodissolution rates [18]. It is therefore plausible that Fe could be an important ion in glacial meltwater.

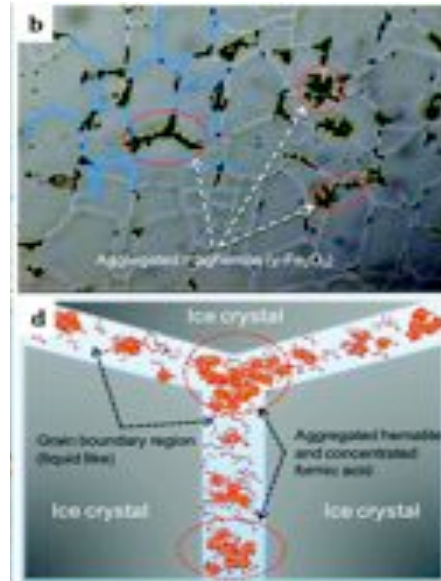


**Figure 9** [18]. The Ice-Grain Boundary: Researchers have observed photochemical reactions in the ice-grain boundary as a result of low pH levels and significant exposure to UV light.

Understanding the ice-grain boundary is significant because it explains the journey of iron oxide into soluble iron  $\text{Fe}^{2+/3+}$ , which are the species detectable by the analytical methods used in this project.

## Methods

### *Sampling Approach and Locations*

Field and lab techniques were used to characterize metal ion concentrations in snow, ice, and water samples from the Nisqually Glacier and River. This study focused on collecting preliminary data in the field with portable meters and reagent kits, and applying the data to metal ion concentrations found in the lab-analyzed samples. Field maps were created using Geographic Information Systems (GIS) software, which can be viewed in Figure 8. Sampling locations were selected with regard to convenience, safety, and relevance.

### *Field Methods*

Hardness was determined using a drop titration test kit, while iron was detected using a color cube test kit (Hach Hardness and Iron Color Cube Test Kit, Model HA-95A). Nitrate was tested using a color disc method (Hach Nitrate Test Kit, Model NI-14). A hand-held meter calculated pH, conductivity, ORP, and TDS at each sampling site (Myron L Company Ultrameter II 6PFC<sup>E</sup>). The two detecting probes were rinsed with sample water three times and held under water for 30 seconds without aeration before readings were taken. Additionally, a hand-held spectrophotometer (Hach 2100- Turbidimeter) was used to calculate turbidity of the water.

Water samples were collected at each sampling site in 50 mL clear, plastic Nalgene bottles. Each sampling bottle was thoroughly washed with sample water three times before a final volume was collected. For sample storage, 3 drops of trace metal grade HCl (Fischer Lot # 4111100) were added to each sample, creating a 0.035M environment. The HCl reagent was added to prevent the organic carbons from consumption by microorganisms. Sample bottles

were labeled and covered with foil to prevent photochemical reactions. Water samples were stored in a refrigerator while snow and ice samples were stored in a freezer.

### *Inductively Coupled Plasma-Atomic Emission Spectroscopy (ICP-AES)*

ICP-AES conducted full-metal surveys for water and digested samples located at the STAR lab at the Ohio Agricultural Research and Development Center. The filtered sample was injected into the instrument, where the sample interacted with an extremely hot argon plasma flame. The sample was atomized into excited state ions, which emitted light in the form of line spectra as the ions fell back to lower energy levels [19]. The brightness and wavelength of the atomic line spectra were detected by the spectrometer, and organized into ion concentration values (Figure 10) [19].

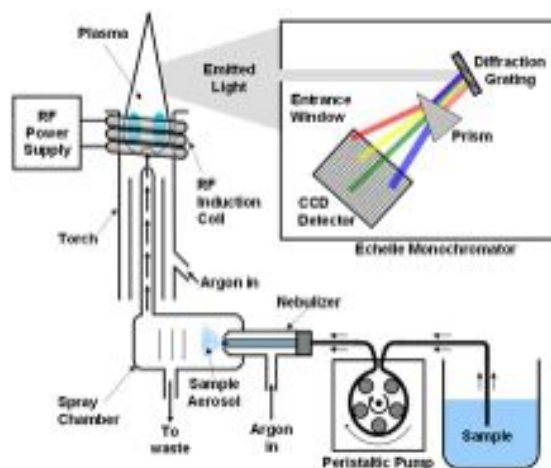


**Figure 10** [19]. The Internal Mechanism of ICP-AES. Liquid samples must be filtered, and solid samples must be digested for successful sample reading.

ICP-AES (Teledyne Leeman Labs Prodigy Dual view ICP) is sensitive to 10 ppb. The bathophenanthroline colorimetric analysis performed was slightly more accurate than ICP-AES, and was easily performed in the lab. To 10 mL of each water sample, 0.5 mL of hydroquinone (Fischer) (a reducing agent) was added to ensure all free Fe species are in the  $\text{Fe}^{2+}$  form, followed

by the addition of 0.5 mL acetate buffer (Fischer) to maintain a pH of 4 in solution. 1 mL of a 50/50 solution of bathophenanthroline (Fredrick Smith Chemical Company Lot # T1) and ethanol (Pharmco AAPER) was added to chelate the  $\text{Fe}^{2+}$  ions, creating an evenly distributed red complex throughout the sample (Figure 11). 2 mL of a 50/50 solution of isoamyl alcohol (Fischer) and dichloromethane (Fischer) was added as non-polar solvent to concentrate the bathophenanthroline-Fe complex in the bottom of the sample tube. The red complex was carefully pipetted into cuvettes for UV-Vis analysis. Absorbance values of the red complex were taken using a UV-Vis machine (Perkin Elmer instruments, Lambda 40 UV/VIS Spectrometer), and inserted into a calibration curve equation to solve for Fe concentration. This assay is described in Figure 11.

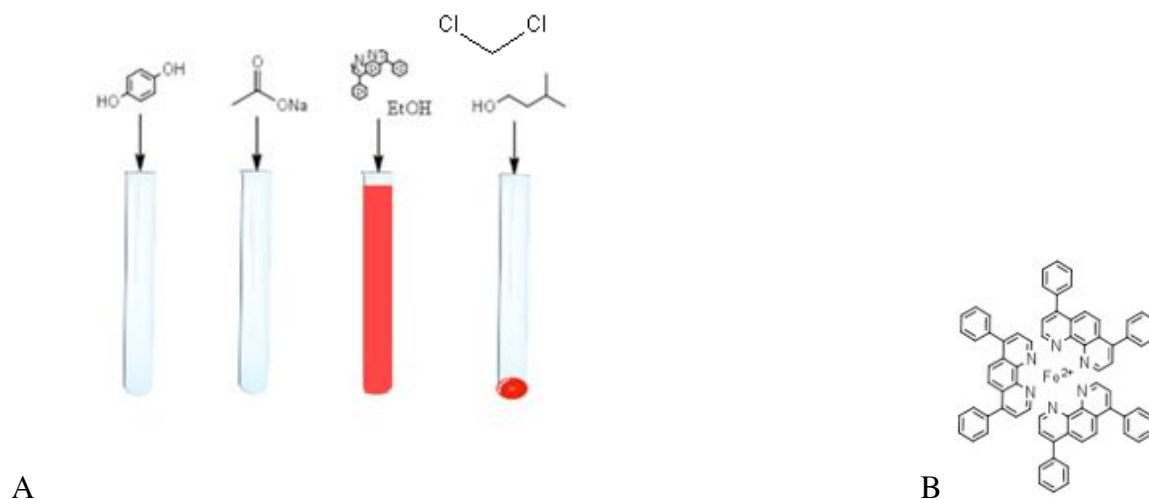


**Figure 11:** Colorimetric Analysis of Fe Concentration Using a Bathophenanthroline Assay. A) Addition of 0.5 mL hydroquinone (reducing agent) to 10 mL of water sample, followed by 0.5 mL acetate buffer at pH 4. A solution of 0.5 mL bathophenanthroline and 0.5 mL EtOH chelates the free  $\text{Fe}^{2+}$  ions, creating a red complex (B). A solution of 1.0 mL dichloromethane/1.0 mL isoamyl alcohol (non-polar solvent) is added to concentrate the bathophenanthroline-Fe complex.

## Results and Discussion

### *Introduction*

Predicting the onset of jökulhlaups is difficult due to a lack of understanding the signals of glacial meltwater stagnation and conditions that may lead to outburst flooding. Understanding the causes for glacial meltwater storage, and measuring the flow of jökulhlaups would provide researchers important information for determining conditions that may lead to events. The goal of this project was to do a complete survey of water chemistry associated with glacial meltwater to find predictors of flow and thus potential signals of water retention. Herein, a signal is defined as a solute that directly emanates from the glacier and could be used to monitor glacial output. A non-signal is a solute dissolved in water that is common in all locations on the mountain, or ubiquitous. A geochemical analysis of the Nisqually Glacier was conducted by collecting snow, ice, water, and debris samples along the glacier. Surface and deep crevasse ice, Nisqually River water, surface stream water, water from a flooded crevasse, and surface debris were amongst these samples. Items from the summit (hoarfrost, fumarole residue, and ice cave snow) were also collected and analyzed as a geochemical baseline for Mount Rainier. Ice, snow, and water samples from the Emmons glacier were collected as a control variable against the Nisqually. Snow samples were also collected from the Paradise Glacier to compare with the Nisqually. All samples were collected following NPS sampling protocol. Sampling sites were strategically chosen to observe how the measured chemical signals diluted downstream from the Nisqually terminus by non-glacially fed tributaries. Water samples collected near the terminus contained non-diluted signals, as there were zero tributaries feeding into the river between the sampling location and the terminus. Three major snowpack tributaries were sampled downstream to determine which signals were representative, or non-representative, of snowpack melt when observing the dilution of glacial signals along the Nisqually River.

## Sampling Locations

GPS coordinates were taken for each sampling location, and are listed below in Table 3.

**Table 3:** GPS Coordinates for Sampling Sites in Mount Rainier National Park  
UTM – NAD83

Sample Locations	Northing	Easting	Date/Time
<b>Nisqually River and Tributaries</b>			
NR 8 (Kernahan Bridge)	5177236	577808	7/17/12 8:09AM
NR 12 (Sunshine Point)	5176804	582216	7/17/12 9:23AM
NR 13 (Mile Marker 5)	5177582	590235	7/17/12 10:05AM
NR 14 (Longmire)	5177873	590944	7/17/12 10:44AM
NR 15 (snowmelt stream on Eagle Point trail)	5177874	591563	7/17/12 11:10AM
NR 16 (Carter Falls)	5179896	592408	7/17/12 12:59PM
NR 17 (Narada Falls, snowmelt)	5180956	595724	7/17/12 13:22PM
NR 18 (Christine Falls, snowmelt)	5181527	593195	7/17/12 14:09PM
N GB (Nisqually Glacier Bridge)	5181616	594481	8/8/12 16:42PM
NR TERM (Nisqually Glacier Terminus)	5182573	595391	8/8/12 15:00PM
<b>Nisqually Glacier</b>			
Snow Core	5185516	596063	8/7/12 16:30PM
Water-filled Crevasse (deeper than 12 m)	5185516	596063	8/3/12 13:03PM
Surface Stream Water (through trail of elevated, brown/rocky debris)	5184833	596243	8/7/12 15:33PM
Surface Snow	5184833	596243	8/7/12 15:33PM
Surface Debris	5184833	596243	8/7/12 15:33PM
<b>Emmons Glacier</b>			
Pond Ice (dead/stagnant ice)	5194664	601868	8/3/12 19:00PM
Surface Snow (on top of stagnant ice)	5192084	600349	8/4/12 12:30PM
Glacial Water (from outflow)	5193715	601100	8/4/12 18:12PM
<b>Paradise Glacier</b>			
Paradise River Water (opening in snowfield directly below glacier ice)	5185531	598006	8/8/12 17:00PM
Surface Snow (adjacent to river)	5185531	598006	8/8/12 17:00PM

*Physical and Chemical Measurements*

Temperature, conductivity, ORP, pH, and TDS data were collected at each sampling site using the hand-held meter (Table 4). The goal of taking these measurements was to determine which measurements were signals for the Nisqually’s glacial outflow. A complete list of data may be found in Appendix I.

**Table 4.** Temperature, Conductivity, ORP, pH, TDS and Turbidity Measurements of Nisqually River Sampling Sites and Snowmelt Tributaries: Samples were collected 7/17/12.

Sampling Locations	Distance from Terminus (km)	Temperature (°C )	Conductivity (uohms/cm)	ORP (mV)	pH	TDS (mg/L)	Turbidity (NTU)
NR 8 (Kernahan Bridge)	18.563	8.4	29.34	323	6.55	22.63	93.0
NR 12 (Sunshine Point)	14.935	8.5	32.18	329	6.50	20.77	117
NR 13 (Mile Marker 5)	7.876	7.5	18.04	335	6.09	11.50	107
NR 14 (Longmire)	7.190	7.6	19.04	308	6.29	12.06	138
NR 16 (Carter Falls)	4.711	8.4	51.48	315	6.00	30.20	190
Snowmelt Tributaries Along the Nisqually River							
NR 15 (snowmelt stream on Eagle Point trail)	6.812	9.1	30.20	255	6.39	152.40	0.00
NR 17 (Narada Falls, snowmelt)	2.348	6.0	34.02	292	6.44	22.32	0.03
NR 18 (Christine Falls, snowmelt)	3.029	10.1	46.20	289	6.41	29.00	0.00

Temperature, pH, turbidity, and metal ion concentrations were considered to be signals for characterizing glacial outflow. Identified signals provide a distinction between glacial meltwater

and snowmelt, which assist in determining how chemical signals from the glacier dilute downstream from the glacial terminus. Temperature is higher in the snowmelt tributaries than glacial meltwater, indicating escalated snowmelt presence in the river as the river water temperature increases. pH is generally consistent between snowmelt and glacial melt, but a drastic change in pH would be indicative of a hydrogeological shift in the glacier [15]. Turbidity experiences a general decrease in value as the clear snowmelt tributaries dilute the glacial meltwater downstream from the terminus. Glacial melt is turbid from rock flour, but other sources including silt from the streambed may contribute to the turbidity, which varies the level at each site.

Metal concentration was examined in all sampled water. The metals represent an entirely new suite of analytes examined in this study, which to current knowledge, has not been measured in previous work. Samples collected at each site were measured in triplicate for the new suite of analytes; of the 28 metals measured, Na, Al, Mn, Mg, Ca, and Fe were identified as potential signals due to their high concentration, or statistically significant difference in value between glacial and snow melt (full suite Appendix II). Comparisons in the concentration of individual metals between glacial melt and snowmelt were made. In addition, the dilution of potential signals (metal concentrations) was studied by having a wide number of sampling points downstream. A strong signal would have a significant difference in concentration between glacial and snow melt, while a weak signal would not. Though Na was found in high concentrations in the glacial meltwater, it was also found in high concentrations in the snowmelt (Figure 12). Therefore, Na is ubiquitous over Mount Rainier and is not a signal for glacial outflow. Each of the seven circles represents an average of triplicate measurements taken with inductively coupled plasma-atomic emission spectroscopy (ICP-AES). The bars around the

circles indicate standard deviations. The dashed line is the average  $\text{Na}^+$  concentration in the snowmelt tributaries, while the red lines indicate the standard deviation in the snowmelt.

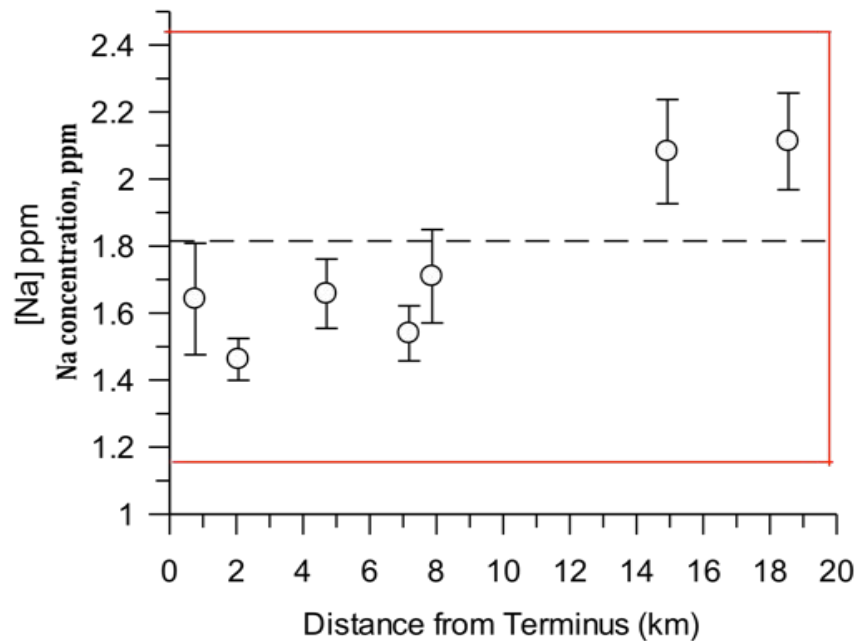


**Figure 12.** Sodium ( $\text{Na}^+$ ) concentration as a function of distance from the Nisqually Terminus.

It is presumed based on known chemical stability that the elevated aluminum levels are from  $\text{Al}_2\text{O}_3$  present in the rock flour.  $\text{Al}_2\text{O}_3$  is a major component of minerals in the earth's crust, and is expected due to the strong tendency of  $\text{Al}^{2+/3+}$  ions to oxidize. The ICP-AES atomizes all species in the sample, which would transform all forms of Al into free Al ions detectable by the ICP's sensor [20]. Al is found in higher concentrations in glacial melt than snowmelt. Therefore, Al appears to be a strong signal in Figure 13, but may not be as unique to the Nisqually as the other signal ions. Also, measurement is logistically more difficult because detection requires more expensive plasma atomization analytic instruments.

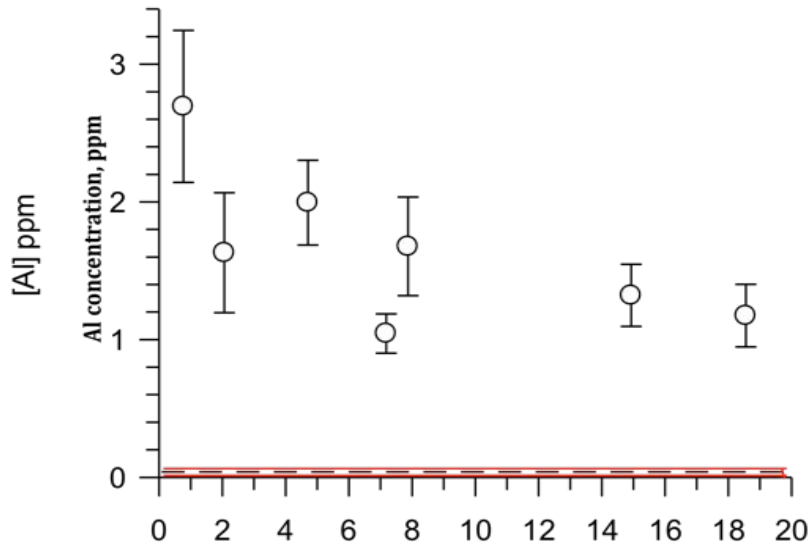


**Figure 13.** Aluminum at Distances from the Nisqually Terminus.

Manganese (likely from  $\text{MnO}_{2(s)}$  or  $\text{Mn}^{2+}$ ) was also found in significantly higher concentrations in glacial meltwater. Compared to alumina, manganese is chemically less abundant and could be defined as a unique signature ion for the Nisqually Glacier (Figure 14) [3]. Mn was not detected in snowmelt, and is unique to the Nisqually's glacial outflow. Decrease in the concentration downriver from the glacial terminus is attributed to dilution by tributary inflow or precipitation by oxidation. An additional removal mechanism was postulated due to the higher rate of decay compared to other metal ions.

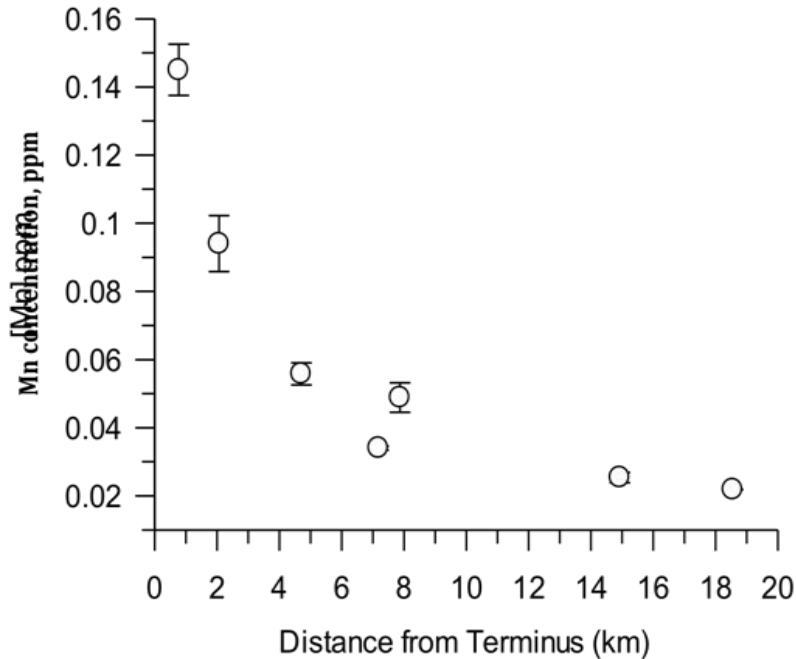


**Figure 14.** Manganese concentration at Distances from the Nisqually Terminus.

Magnesium (likely found as  $Mg^{2+}$ ) was also tested by ICP-AES. Mg was expected due to its solubility compared to other metal oxides. Thus, it was not surprising that Mg was detected in appreciable amounts in both glacial melt and snowmelt. Although Mg was observed at higher concentrations in glacial outflow, the element was considered to be a weak signal for glacial outflow (Figure 15) due to widespread abundance. Decay of signal is generally consistent with the other metals observed. Due to magnesium's solubility it is presumed that dilution is the mechanism for the decrease in concentration downstream. Andesite lava flow is the primary rock type at Mount Rainer, and typically, andesite has depleted levels of magnesium [3].

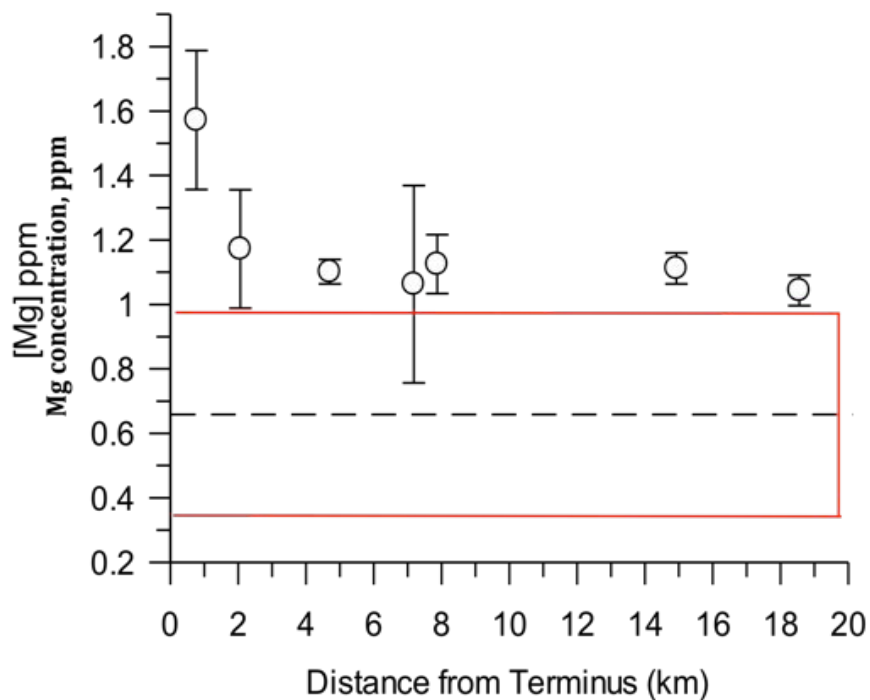


**Figure 15.** Mg concentration at Distances from the Nisqually Terminus.

Calcium (presumed to be in the dissolved state as  $\text{Ca}^{2+}$ ) was more concentrated in glacial melt than snowmelt, but not to the same extent as other measured metals. There was a notable increase in calcium concentration between 8 km and 16 km downstream from the Nisqually terminus that is likely the result of a Ca source in Longmire Meadow (Figure 16). Ca may be used as a signal for glacial outflow, but it is not a strong signal due to the unresolved spike in calcium concentration.

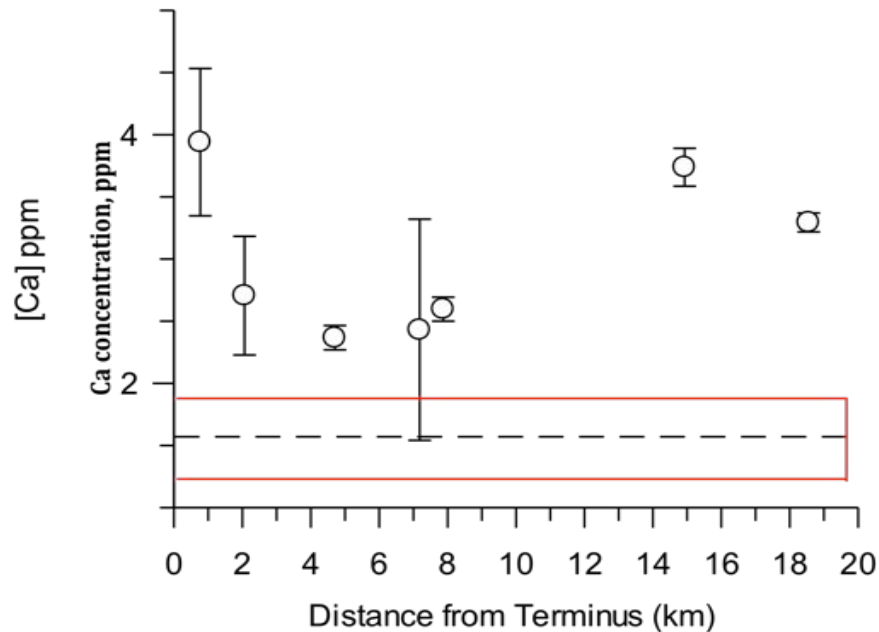


**Figure 16.** Ca concentration at Distances from the Nisqually Terminus.

### *Iron*

Iron was determined to be one of the strongest signals for glacial outflow, as it was an order of magnitude more concentrated in glacial melt than snowmelt during the summer months (Figure 17). Winter samples showed no concentration of Fe by the bathophenanthroline colorimetric method, with and without acid. Of particular interest is the form in which this iron is present. Substantial interest from an ecological and geochemical perspective would be found if Fe is in the free ionic form. Thus, particular emphasis is placed in the speciation of iron. ICP-AES does not distinguish between free (soluble) iron and present iron oxides. As a result, a colorimetric assay was performed that only detects dissolved iron ( $\text{Fe}_2\text{O}_3$  or  $\text{Fe}^{2+/3+}$ ), which confirmed that all the iron detected in the meltwater was in the dissolved ionic form. It is possible, but unlikely, that the acid added to the water samples during storage degraded  $\text{Fe}_2\text{O}_3$  species into free iron. A concentration of 0.5M HCl is required to degrade  $\text{Fe}_2\text{O}_3$  species, and

these samples had a concentration of 0.035M HCl. A study by Kanungo et al. observed the degradation of iron oxide at various concentrations of HCl (Figure 17)

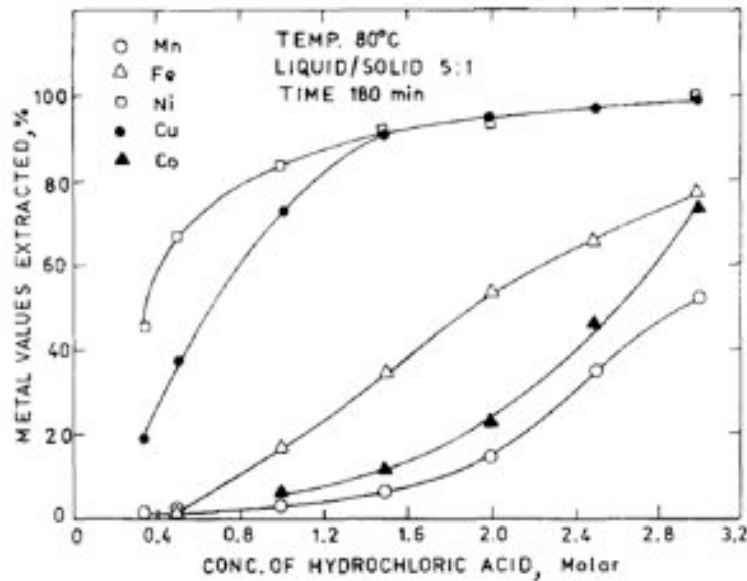


**Figure 17 [21]:** Extraction of Metals at various HCl concentrations. Metal oxides are degraded with increasing HCl concentration, allowing metal ions to become available for extraction. More specifically, iron oxide begins degradation around 0.5 M HCl.

The presence of free iron is unusual due to the fact that iron readily forms oxides and hydroxides under aerobic conditions in natural water. Iron is a trace nutrient despite its abundance in the crust. Detection of free soluble iron was considered to be a strong signal as the amount of similar iron in snowpack meltwater was typically low or non-detectable. The presence of free iron in glacial meltwater points to chemical or photochemical reactions that dissolve iron oxides in ice grain boundaries.

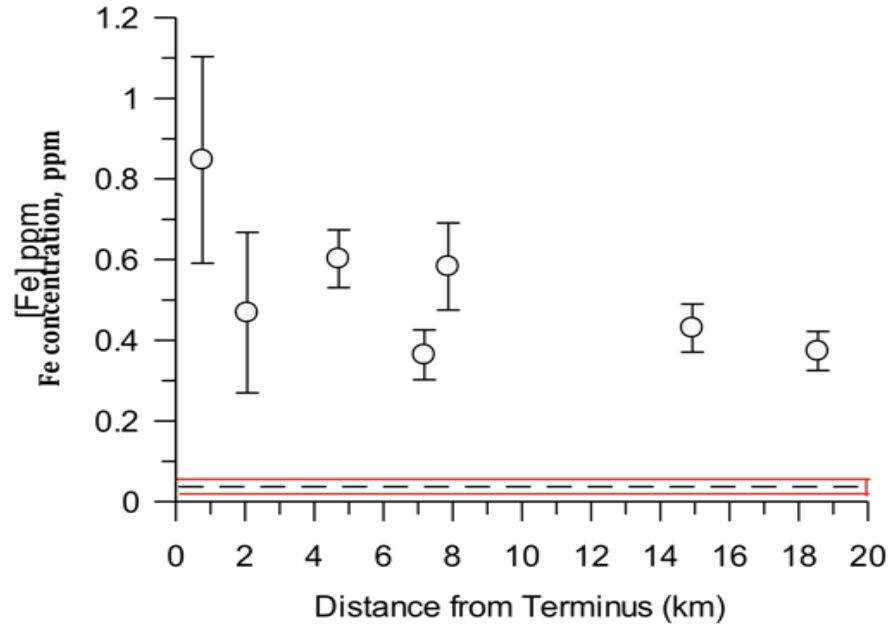


**Figure 18.** Fe concentration at Distances from the Nisqually Terminus.

The significance of the difference in various metal ion concentrations was examined using a t-test to calculate the probability of glacial melt and snowmelt containing the same concentrations of metal ions (Table 5).

**Table 5.** t-test Comparing Ion Concentrations in Glacial meltwater with Snowmelt. p represents the probability of the glacial melt and snowmelt having the same ion concentration values.

Element	t	p
Fe	9.26	<0.001
Al	5.28	0.000
Ca	4.65	0.001
Mg	3.49	0.006
Mn	3.00	0.013
Na	0.236	0.818

The probability results signify that glacial meltwater has significantly higher dissolved Fe, Al, Ca, Mg, and Mn content than snowmelt. In other words, the probability of glacial melt and snowmelt containing the same ion concentrations is negligible, indicating these ions are signals for glacial melt. Na is not statistically different between glacial meltwater and snowmelt, which is visible by the standard deviation of Na concentration in snowmelt encompassing the values of Na concentration in the glacial melt (Figure 12).

### *Iron Speciation Analysis*

As noted above, Fe was analyzed with a bathophenanthroline colorimetric assay in addition to ICP-AES in order to determine the chemical state. The colorimetric assay uses an iron chelator that binds only free iron ions. The method lacks a mechanism to dissolve the metal oxide, so a positive result is due to free iron. The iron concentrations from the colorimetric assay were similar to the results from ICP-AES, indicating the iron was in free dissolved form. A paired t-test was used to evaluate individual differences in values from two different methods. The following equation calculated the standard deviation of each of the differences [22]:

$$s_d = \sqrt{\frac{\sum (d_i - \bar{d})^2}{n - 1}}$$

The average of the differences for each of the two values is represented by  $\bar{d}$ , the difference between the two values for each sample ( $d_i$ ), and the number of compared sample couples, or degrees of freedom, (n) [22]. The t value is then calculated using [22]:

$$t = \frac{\left| \bar{d} \right|}{s_d} \sqrt{n}$$

The value for  $\bar{d}$  is ensured to be positive by taking the absolute value, which guarantees a positive t value [22]. Degrees of freedom for the tests are compared to the t value using a confidence level table to afford the percent confidence of the values being the same [22]. A paired t-test comparison of iron concentrations for nine samples using ICP-AES analysis and a bathophenanthroline colorimetric analysis afforded 95% confidence that the two methods produced identical values. The test was completed in Excel (Table 6).

**Table 6:** Paired t-test Comparison for Fe concentration in Samples Using ICP-AES Analysis and a Bathophenanthroline Colorimetric Analysis. ICP values for all samples except Snow from the Paradise Glacier contain averages of triplicate data. NR# samples are from the Nisqually River (locations described in Table 3). The bathophenanthroline Fe concentration values represent one measurement.

Sample	ICP (ppm)	Bathophenanthroline (ppm)	d	di
NR8	0.373	0.314	0.059	0.03674037
NR12	0.43	0.839	-0.409	0.07635397
NR13	0.583	0.743	-0.16	0.000746504
NR14	0.364	0.39	-0.026	0.011380148
NR16	0.602	0.582	0.02	0.023310504
GB	0.469	0.699	-0.23	0.009471615
T1	0.8470	1.28	-0.433	0.090193437
Snow from the Paradise Glacier	0.0453	0.07	-0.0247	0.0116592
NR17	0.025	0.0154	0.0096	0.020242966
		d bar	-0.132677778	0.187115845
		t	2.127202714	
			95% the same	

Bathophenanthroline values read higher than ICP values in a majority of the comparisons, which may be attributed to calibration differences. These differences are not statistically significant, as the t test confidence interval of 95% indicated that the Fe concentrations were statistically the same for both methods. It is possible but unlikely that the acid used for sample storage degraded Fe<sub>2</sub>O<sub>3</sub> species into free Fe detectable by bathophenanthroline. Further work in understanding the chemistry of iron is needed.

*Variables that Affect Fe Concentration*

Analysis of results from ICP-AES testing showed soluble Fe concentration to vary significantly between ice, snow, and water samples, and to gradually dilute along the Nisqually River (Table 7).

**Table 7.** Fe concentration in Various Sampling Locations: Each Fe concentration represents one measurement detected by ICP-AES.

Site	Fe concentration, ppm
Nisqually Glacier Ice	1.5005
Nisqually River: Terminus	0.6030
Nisqually River: Kernahan Bridge	0.3176
Nisqually Glacier Surface Snow	0.0372

It was accurately predicted that Fe would be most concentrated in the ice for reasons not concretely understood. Iron concentration decays downstream from the terminus as the glacial meltwater becomes diluted with snowmelt containing minimal iron. Understanding the dilution

of Fe along the river will allow researchers to accurately measure glacial outflow in more accessible areas downstream from the terminus.

The question remains: do glacial discharge and Fe concentration relate, and further, do glacial discharge and temperature relate? Figure 19 illustrates Fe concentration of Nisqually River samples collected from five locations downstream of the glacial terminus. Samples were gathered on adjacent days with extremely similar weather conditions.

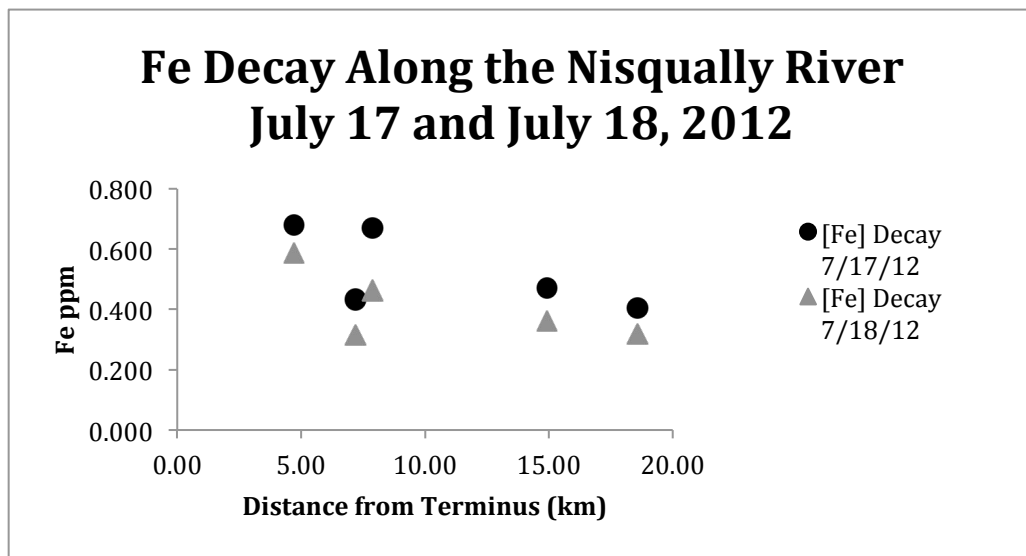


**Figure 19:** Comparison of Fe Concentration Decay Along the Nisqually River Between July 17 and July 18, 2012. Each sample point represents one measurement produced with ICP-AES analysis.

A clear decrease in Fe concentration with increasing distance from the terminus is visible, which is attributed to dilutions from snowmelt tributaries that feed into the Nisqually River. Also noted is the slight decrease in Fe concentration on July 18<sup>th</sup> from July 17<sup>th</sup>; discharge rates are almost identical for both days, but the water temperature was warmer on the 18<sup>th</sup>. Warmer water could be a result of higher snowmelt composition, which explains the lower Fe concentration.

In an effort to relate Fe concentration at locations along the Nisqually River with river flow, data was analyzed from a toll station situated at Longmire that measures discharge at

fifteen-minute intervals. These measurements may be matched with samples collected at Longmire at three different times in order to study the relationship between Fe concentration and discharge rate (Figure 20).

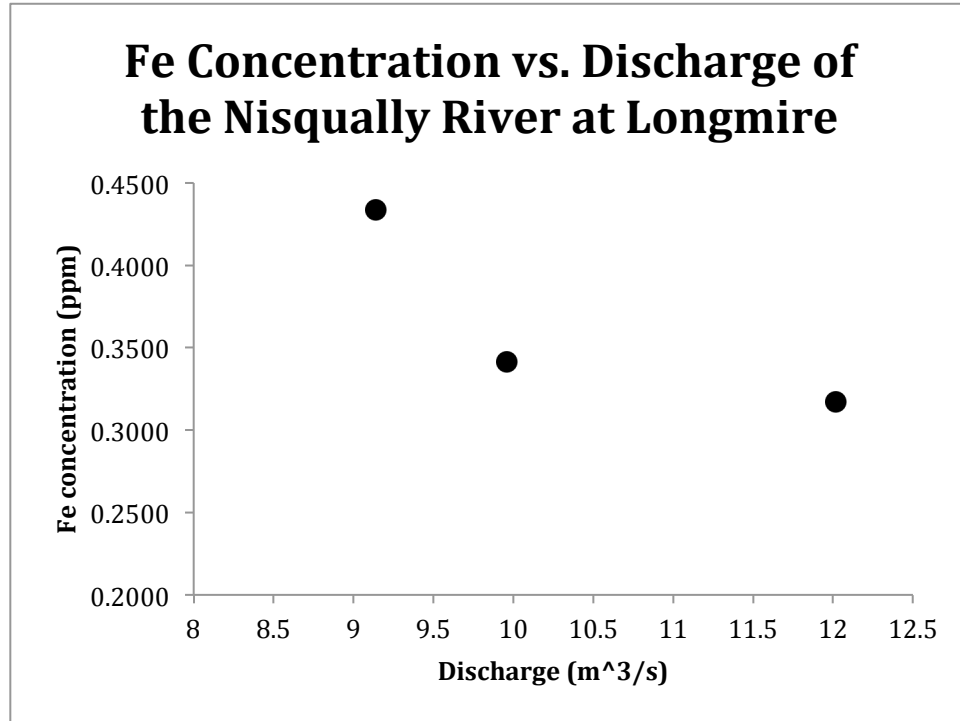


**Figure 20:** Fe Concentration at Various Discharge Rates on the Nisqually River at Longmire. Each data point represents one measurement produced with ICP-AES for Fe concentration. Discharge data was measured with a toll station on the Nisqually River, and attained from Mount Rainier National Park’s Scott Beason.

According to Figure 20, Fe concentration decreases as discharge rate increases. This finding follows suit with Figure 20, as an increase in water temperature corresponds to lower Fe concentration due to a higher contribution from snowmelt. Higher overall melt also signifies an escalated discharge rate. Therefore, lower Fe concentration corresponds to a higher discharge rate. This relation also follows suit with Figure 21, which anticipates lower Fe concentration and higher discharge rates for the summer melt season [15].

	High Flow	Low Flow
High Fe	No stagnation	Winter normal
Low Fe	Summer normal	Stagnation

**Figure 21:** Glacial Outflow Status According to Flow vs. Fe concentration mid-day. High levels of Fe concentration and flow velocity represent a moving glacier, while low levels of Fe concentration and flow velocity indicate a stagnant glacier. High flow and low Fe concentration are standard for a summer day, while low flow and high Fe concentration are standard for a winter day.

This potential predictive model is an untested hypothesis, and requires sampling over the course of an entire year to fully observe the changes in iron concentration with varying temperature and flow velocities.

### *Temperature and Discharge Rate*

Temperature and discharge rate appear to be related through comparisons made above, yet the graphical relation between the two variables does not appear strong. At various times, temperature and discharge measurements were recorded on the Nisqually River at Longmire (Figure 22). Further sampling across a wider range of seasons would be important to assess the correlation between temperature and discharge.

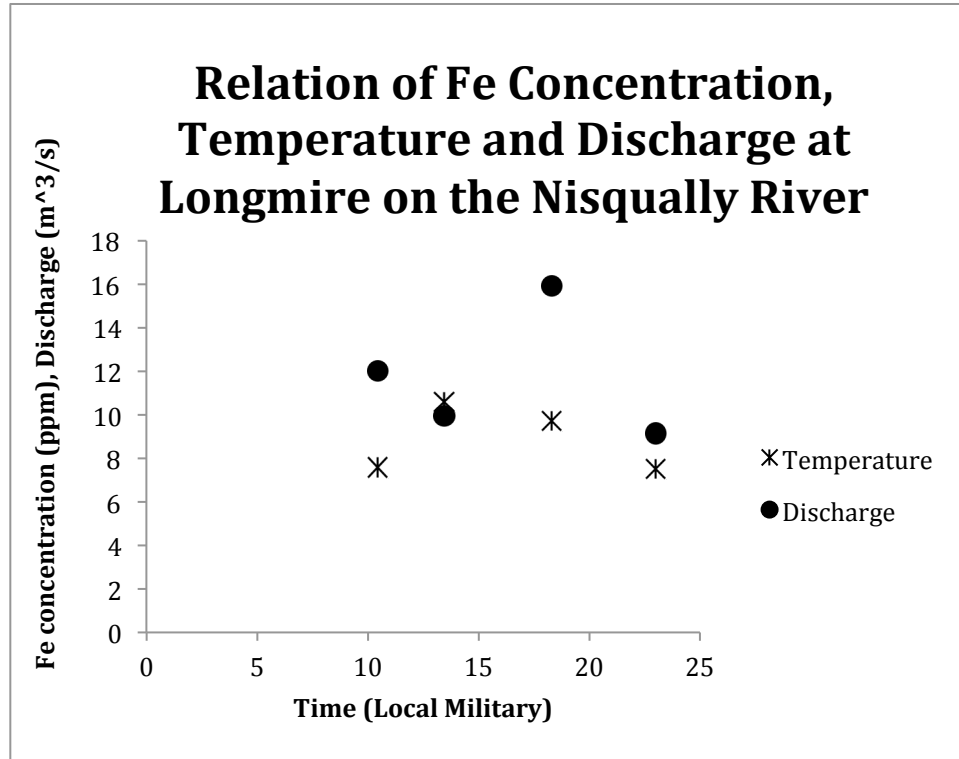


**Figure 22.** Relation of Fe Concentration, Temperature and Discharge at Longmire. Temperature data was recorded using a hand-held meter, and discharge rates were measured by a toll station along the Nisqually River. Each data point represents one measurement.

It was assumed that water temperature and discharge would be directly related, but Figure 22 indicates a slightly more complex relation. The lag between temperature rise/drop and discharge rise/drop may be attributed to the longer time interval for discharge to travel from the terminus to Longmire than that of the water temperature [3]. Water temperature may also change more rapidly due to heat absorption from sunlight and warmer water from snowmelt tributaries [3].

#### *Potential Origin of Free Metals in Glacial Meltwater*

The high concentrations of free metals in the collected samples, notably iron, were distinguished results. A key research question asks why the iron was found in the soluble free form. There are three potential reasons. First, the iron may have been dissolved by the acid

preservative added during sample collection. Second, the iron may be solubilized by physiochemical processes within the glacial system. A Korean research team explained the conversion of insoluble metal complexes into soluble metal ions by exploring the interworking of ice crystals. The crystalline ice pushes foreign particles into a vein-like network called the ice-grain boundary between the ice crystals [18]. Ions become highly concentrated in this boundary with acidic species, including oxalic acid [18]. Exposure to UV light over the course of years in a highly acidic environment drives oxidized species to undergo photochemical reactions [18]. More specifically,  $\text{Fe}_2\text{O}_3$  undergoes photoreductive dissolution in the ice-grain boundary, producing free  $\text{Fe}^{2+/3+}$  ions [18]. The free ions become soluble and are detectable by analytical techniques (i.e. ICP-AES). Third, elevated metal ion concentrations may emanate from thermal springs or other vents that underlie the glacier [3]. Similar springs are located at Longmire Meadow, which lead to an uptick in concentration in the Nisqually River.

#### *Anthropogenic Metal Sources and Notes on Sampling*

During the course of study samples were taken near Glacier Bridge. It was found that one sample taken on the downstream side of the bridge during the summer exhibited high levels of metals that were not detected at any other site throughout the study. Specifically, elevated levels of copper and chromium were observed in the downstream sample. Calcium, phosphorous, and aluminum were also elevated. Upstream samples did not have elevated levels of these compounds, and samples taken during the late Fall also had standard levels of metals. Based on these observations, it is hypothesized that high levels of traffic that occur during the summer lead to run-off that locally contaminates the Nisqually River. As a result, it is

recommended that sampling be done upstream of the bridge or far downstream from Glacial Bridge where metals from vehicles will not lead to variable data.

**Table 8.** Comparison of a Contaminated Water Sample from Glacier Bridge to a Non-Contaminated Water Sample. Contamination may be a result of roadbed runoff or material dispensed into the river. To help prevent contaminated samples, conduct sampling upstream of bridges.

Glacier Bridge Samples	P (ppm)	Ca (ppm)	Al (ppm)	Cu (ppm)	Cr (ppm)
Contaminated	9.836	30.571	7.813	35	2
Non-Contaminated	0.632	3.153	2.111	7	<0.200

### *Ecological Implications*

Glaciers may be a significant source of trace nutrients for ecosystems across the globe. Some of the most bioactive areas reside directly downstream of glacial meltwater, or in the same watershed [3]. Representations of chlorophyll activity have been developed for the Alaskan Gulf, which is known to be one of the world’s most bioactive and biodiverse regions. Chlorophyll is an essential fuel source for organisms, and more specifically, zooplankton and phytoplankton, which are staple food sources for larger species and animals [3]. Increased chlorophyll abundance would provide plankton with more nutrients, which in turn would increase the plankton population. A larger plankton population accounts for a larger food source for animals, which increases overall bioactivity. Chlorophyll abundance increases as the temperature rises during the year (Figure 23). Detection of high concentrations of free iron in glacial meltwater is a potentially exciting finding that could further link geochemistry and aquatic ecosystems.

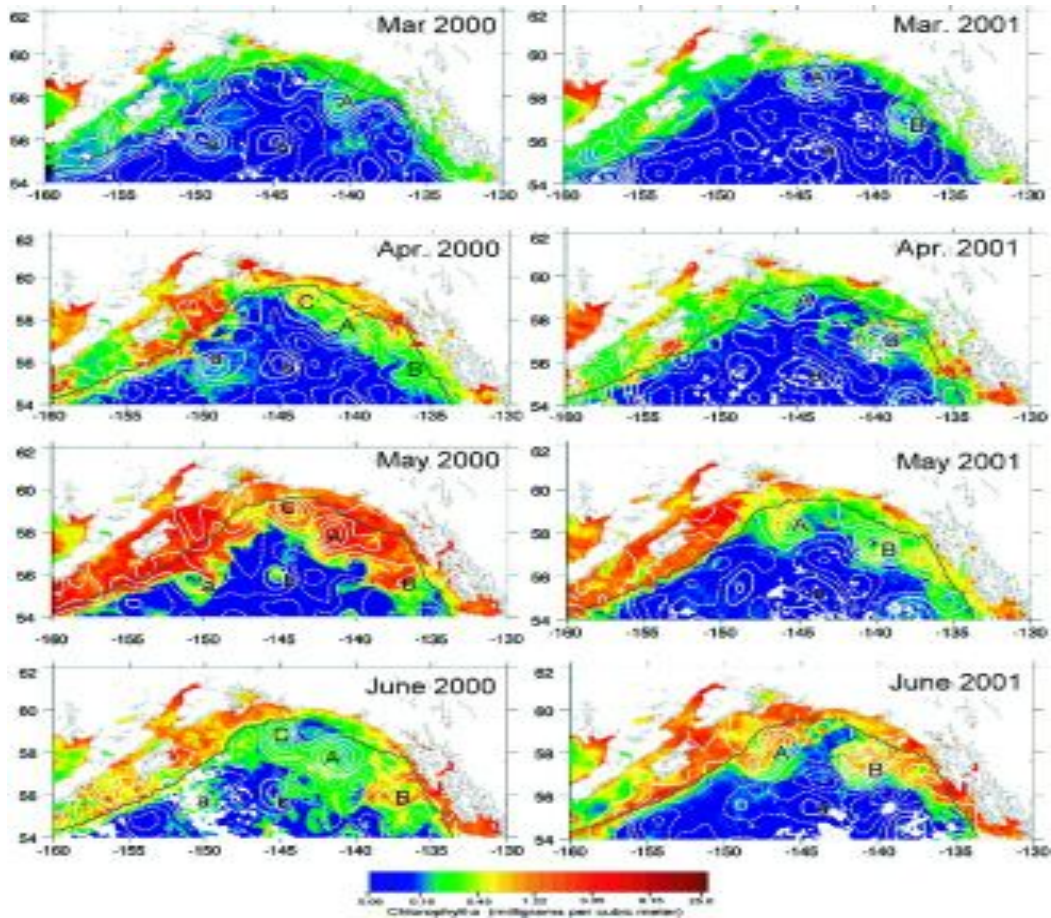


**Figure 23** [23]. Chlorophyll Abundance in the Alaskan Gulf. Blue regions indicate lower chlorophyll abundance, while red regions indicate higher chlorophyll abundance.

Glaciers experience higher elution rates during the summer as a result of increased temperature [15]. Fe concentration would therefore elute at higher concentrations during the summer than the winter, which directly correlates to chlorophyll abundance patterns. Fe is a staple nutrient for nearly all ecosystems, and is likely to be a significant trace nutrient for chlorophyll in the Alaskan Gulf. It is possible that Fe concentration from glacial outflow is an essential nutrient for chlorophyll, and further, an essential nutrient for bioactivity [3]. Considering the loss of our glaciers raises the question as to what implications ecosystems like the Alaskan Gulf will experience; it is possible that Fe is a substantial driver of these ecosystems.

## References

- [1] Poore, R.; Williams, R.; Tracey, C. Sea Level and Climate: Fact Sheet 002-00. USGS 2000.
- [2] Jansson, P.; Hock, R.; Schneider, T. The concept of glacier storage: a review. *Journal of Hydrology* 282 (2003) 116-129.
- [3] P. Edmiston, personal communication, August 2012 –March 2013.
- [4] Benn, D.; Evans, D. (1998). *Glaciers & Glaciation*. London: Arnold Publishing.
- [5] Iceland on the Web. Iceland Nature: Glaciers in Iceland. Retrieved from [http://iceland.vefur.is/iceland\\_nature/glaciers\\_in\\_iceland/](http://iceland.vefur.is/iceland_nature/glaciers_in_iceland/)
- [6] TURDUS.net. Jökulhlaup: Glacial Outburst Flood. Retrieved from <https://notendur.hi.is/thorstur/science/jhlaup/jhlauputor.htm>
- [7] G. Wiles, personal communication, November 26, 2012.
- [8] Ford, K. The impacts of climate change at Mount Rainier National Park. *University of Washington*. **2012**, pp. 3-8
- [9] Björnsson, H. Jökulhlaups in Iceland: Sources, Release and Reainage. *Hyper Articles en Linge*. **2012**, pp. 1-14
- [10] University of Iceland Science Institute: Geographics Division. *The Subglacial Lake Grímsvötn*. Retrieved from <http://www.raunvis.hi.is/~alexandr/glaciorisk/jokulhlaup/subglaVolc/vatna/grims/index.html>
- [11] Walder, J.; Driedger, C. Glacier-generated debris flows at Mount Rainier: *Volcano Fact Sheet / Open-File Report 93-124*.
- [12] Heliker, C.; Johnson, A.; Hodge, S. The Nisqually Glacier, Mount Rainier, Washington, 1857-1979: A Summary of the Long-Term Observations and a Comprehensive Bibliography. *U.S. Geological Survey: Open-File Report 83-541*. **1984**.
- [13] P. Kennard, personal communication, January 3, 2012.
- [14] P. Kennard, personal communication, November 27, 2012.
- [15] Anderson, S.; Longacre, S.; Kraal, E. Patterns of water chemistry and discharge in the glacier-fed Kennicott River, Alaska: evidence for subglacial water storage cycles. *Chemical Geology* 202 (2003) 297-312

- [16] Marx, S.; Kamber, B.; McGowan, H. Provenance of long-travelled dust determined with ultra-trace-element composition: a pilot study with samples from New Zealand glaciers. *Earth Surf. Process. Landforms*. **2005**, 30, pp. 699-716.
- [17] Larson, A. The Influence of Geology on the Chemical Composition of Two Washington Rivers. *Northwest Science*. **1982**, 57, pp. 256-266
- [18] Kim, K.; Choi, W.; Hoffmann, M.; Yoon, H.; Park, B-k. Photoreductive Dissolution of Iron Oxides Trapped in Ice and Its Environmental Implications. *Environ. Sci. Technol.*, 2010, 44 (11) pp 4142-4148.
- [19] Analytical Chemistry Laboratory Manual: Inductively Coupled Plasma Atomic Emission Spectrometer (ICP-AES). Concordia Analytical Instrument Laboratory. Concordia College. Moorehead, Minnesota.
- [20] K. Jewell, personal communication, February 15, 2013.
- [21] Kanungo, S.; Jena, P. Studies on the Dissolution of Metal Values in Manganese Nodules of Indian Ocean Origin in Dilute Hydrochloric Acid. *Hydrometallurgy*. **1988**, 21, pp. 23-39.
- [22] Harris, D. Quantitative Chemical Analysis Seventh Edition. pp 58-62 4-2 Confidence intervals 2007 W. H. Freeman and Company.
- [23] William R. Crawford; Peter J. Brickley; Andrew C. Thomas; Mesoscale eddies dominate surface phytoplankton in northern Gulf of Alaska. *Progress in Oceanography*, 2007, 75 (2) pp 287-303.
- [24] Lapo, K.; Todd, C.; Koester, A. Glacial Meltwater Hydrochemistry on Mount Rainier, Washington. *2012 GSA Annual Meeting, Session No. 157*. Booth# 58.

# Appendix 1

Nisqually River (NR) Sample Site # - Sample Day, Nisqually Glacier (NG), Emmons (E), Paradise (P), Water (W), Snow (S), Ice (I)																	
ID	Temp	Conductivity	ORP	pH	TSS	Turbidity (NTU)	Hardness (mg/L)	Iron (µg/L)	Nitrate	Nitrogen	Ammonia	Coordinate System	Time	Date	Notes		
NR 1-1	2.3	31.84	310	5.87	27.52							5182949	59533	UTM - NAD83	7/3/16	closed spot to terminus	
NR 3-1	2.3	33.47	314	6.37	20.20							5182794	59517	UTM - NAD83	7/3/16	above Niqz bridge	
NR 3-1	2.4	35.79	323	6.06	21.18							5182596	595427	UTM - NAD83	7/3/16	above Niqz bridge	
NR 4-1	2.8	29.49	333	5.98	30.90							5183366	595200	UTM - NAD83	7/3/16	above Niqz bridge	
NR 5-1	3.2	38.50	331	5.90	28.75							5182278	595089	UTM - NAD83	7/3/16	above Niqz bridge	
NR 6-1	3.2	29.59	333	5.99	28.85							5182120	594950	UTM - NAD83	7/3/16	above Niqz bridge	
NR 7-1	3.9	28.59	341	5.97	34.70							5181977	594825	UTM - NAD83	7/3/16	above Niqz bridge	
NR 8-2	11.5	36.51	344	6.45	26.20							5172236	577808	UTM - NAD83	11:00am	7/8/16	Kemahap?
NR 9-2	13.0	37.14	331	6.38	26.42	24.00						5176459	581825	UTM - NAD83	1:30pm	7/8/16	1st take out in park
NR 10-2	13.3	36.47	316	6.35	103.20	31.50						5178759	581559	UTM - NAD83	1:45pm	7/8/16	1st take out in park
NR 11-2	13.8	41.80	312	6.22	26.40	38.30						5178874	581309	UTM - NAD83	2:10pm	7/8/16	1st take out in park
NR 12-2	14.3	37.39	323	6.43	25.34	29.49						5176884	582216	UTM - NAD83	3:50pm	7/8/16	1st take out in park
NR 13-2	9.8	20.36	330	6.08	13.17	01.00						5177562	590235	UTM - NAD83	6:15pm	7/8/16	below Long
NR 14-3	9.7	16.39	339	6.20	10.45	01.00						5177873	590944	UTM - NAD83	4:25pm	7/10/16	longtime
NR 15-3	8.3	14.44	339	5.89	12.57	0.20						5177874	591543	UTM - NAD83	5:15pm	7/10/16	min stream on Eagle point
NR 16-3	4	32.07	313	6.43	26.06	01.00						5178986	592409	UTM - NAD83	7:55am	7/13/16	Carter falls takeout
NR 17-4	2.6	43.20	319	5.85	0.00	0.00						5180956	595724	UTM - NAD83	8:35am	7/13/16	Narada Falls - Paradise river
NR 18-4	6.2	21.80	313	6.42	20.00	0.00						5181527	593195	UTM - NAD83	9:10am	7/13/16	Christine Falls
NR 19-4	4.8	19.93	328	6.02	20.63	01 + 2.00						5180707	592979	UTM - NAD83	9:30am	7/13/16	Turb range 210
NR 8-5	8.4	29.34	323	6.55	22.63	91.0, 92.8	1.00	1.00	0.00						8:09am	7/13/16	
NR 12-5	8.5	32.18	329	6.50	20.77	117, 130	1.00	1.00	0.00						9:23am	7/13/16	
NR 13-5	7.5	18.04	335	6.09	13.50	01 + 1.07	1.00	0.00	0.00						10:05am	7/13/16	
NR 14-5	7.8	19.04	308	6.29	12.06	136, 0.00	10 + <1.00	0	0.00						10:44am	7/13/16	
NR 16-5	8.4	51.48	315	6.00	30.20	190, 218	<1.00	<1.00	0.00						11:10am		Marked as 19, hardness start purple
NR 17-5	6	34.02	292	6.44	22.32	0.03, 0.03	0.00-1.00	0	0.00						12:59pm	7/13/16	NO3 more pale yellow than the rest
NR 18-5	10.1	46.20	289	6.41	29.00	0.00, 0.00	0.50	0.00	0.00						1:22pm	7/13/16	Hardness clear purple, NO3 very pale yellow
NR 15-5	9.1	30.20	255	6.39	152.40	0.00, 0.14	0.5	0	0.01						2:09pm	7/13/16	
NR 17-6	7.3	92.70	331	7.30	57.82	0.15, 9.99	0.50	0.00	0.00						10:45am	7/18/16	Marked as Narada, NO3 very pale yellow
NR 18-6	9.7	22.20	306	6.25	14.11	0.20, 9.99	0.50	0.00	0.00						11:15am	7/18/16	
NR 16-6	8.5	33.07	282	6.02	21.66	154, 130	0.25	pink<1.00	0.00						11:54am	7/18/16	
NR 14-6	10.6	51.69	302	6.12	33.83	104, 130	0.25	0.00	0.00						1:45pm	7/18/16	NO3 same as Carter
NR 13-6	11.0	19.74	306	6.23	11.52	127, 0.00	a touch	<1.00 not clear	0.00						2:11pm	7/18/16	
NR 12-6	14.3	22.06	294	6.50	47.29	75.2, 130	1.00	<1.00 not clear	0.00						2:47pm	7/18/16	
NR 8-6	14.4	166.50	301	6.91	100.70	82.6, 130	0.25 magenta	0.25 slight orange	0.00						3:21pm	7/18/16	
NR Van Trump										**	**				10:31pm	8/7/12	Van Trump, suspended sediment
NR 16-7															10:40pm	8/7/12	suspended sed.
NR 14-7	7.5	28.04	330	6.41	18.42										11:04am	8/7/12	comm building, suspended sediment
NR 13-7	7.4	30.32	317	6.58	19.73										11:24pm	8/7/12	Mix Point, suspended sediment
NR 12-7	8.9	31.01	293	6.57	19.97										12:24am	8/8/12	suspended sed.
NR 8-7	10.8	53.44	308	6.52	34.79										11:56pm	8/7/12	suspended sed.
NR TEBH	3.2	15.70	368	6.05	12.16	498, 0.0	0.50 magenta	1	0			5182573	595301	UTM - NAD83	3:06pm	8/8/12	mild + cloudy, above glacier bridge
NR GB	5.1	16.64	317	6.33	10.55	352, 130	0.25 magenta	<1.00	0			5181616	594461	UTM - NAD83	4:42pm	8/8/12	under gb
NG Top core										**	**				7:24pm	8/3/16	
NG Mid core															4:30pm	8/7/16	

ID	Temp	Conductivity	ORP	pH	TDS	Turbidity/Range (NTU)	Hardness (mg/L)	Iron (mg/L)	Nitrate	Nitrogen	Leading	Coordinate_System	Time	Date	Notes
NG Low core													4:30pm	8/7/16	
NGW_surface	2.77	342	5.74	1.76						518516	596563	UTM - NAD83	1:03pm	8/3/16	water filled crevasse deeper than 2 sections of probe (1 section 0.90m)
NGW	1.82	339	6.87	1.13						5184833	596243	UTM - NAD83	3:33pm	8/7/16	surface stream thru trail of elevated, brown/rocky debris
NGS	7.58	365	1.01	4.82						5184833	596243	UTM - NAD83	3:33pm	8/7/16	2 samples
NGDebris										5184833	596243	UTM - NAD83	3:33pm	8/7/16	1 sample
EG1	20.12	332	5.94	12.87						5194664	601868	UTM - NAD83	7:00pm	8/3/16	from Emmons pond
EGS	4.6	384	3.39	15.97						5192084	600349	UTM - NAD83	12:30pm	8/4/16	remnant drift along path
EGW	26.52	303	6.76	17.62						5193715 12	601099.9 7	UTM - NAD83	6:12pm	8/4/16	water from outwash
PR	36.95	297	7.12	24.10									5:00pm	8/8/16	breakthrough in snowfield below ice
PGS	2.03	323	6.45	1.28									5:00pm	8/8/16	adjacent to river site

### Sampling Sites

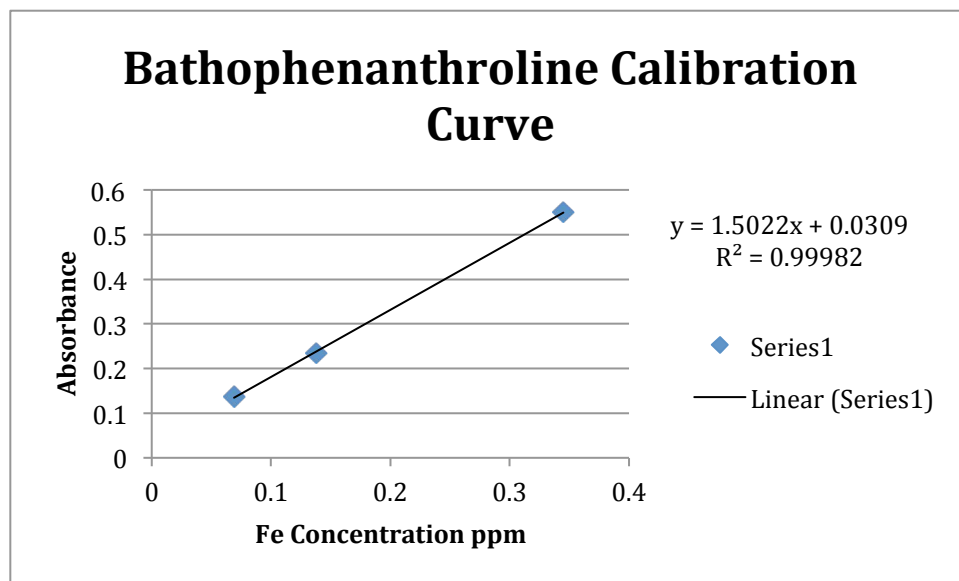
Field Name	Real Name
NR 8	Kernahan Rd.
NR 12	Sunshine Point
NR 13	Mile Marker 5
NR 14	Longmire
NR15	Eagle Point creek
NR16	Carter Falls
NR17	Narada Falls
NR18	Christine Falls
NR TERM1	Nearest site to the terminus
NR GB	Nisqually Galcier Bridge
NG Top core	Surface snow from snow core
NG Mid core	Middle section of snow core
NG Low core	Deepest section of snow core
NGW_surface	Surface water on the Nisqually Glacier through trail of elevated, brown/rocky debris
NGW	Water from a flooded crevasse (deeper than 12 m)
NGS	Pink in color due to algae
NGDebris	Brown/rocky surface debris
EG1	EG1
EGS	EG2
EGW	EG3
PR	PR1
PGS	PG1

Bathophenanthroline Absorbance Values

ID	Abs
T1*	2.108
GB*	1.236
NR18	0.007
NR17	0.054
NR16*	0.264
NR15	0.028
NR14*	0.775
NR13*	1.302
NR12*	1.446
NR8	0.0502
NGI Crevasse	0.475
NGS Crevasse*	0.364
NGW*	0.198
Ice Cave Sum	0.029
Para Glacier	0.136
Para River	0.026
Low Core	0.013
Mid Core	0.028
Topp Core	0.0323
EGS*	0.576
EGI*	2.148
EGW*	0.372

\* diluted samples- original concentration  
out of limit of detection by UV-Vis  
machine

## Appendix 2



ICP-AES Data

Sample ID	P	K	Ca	Mg	S	Al
	ug/ml	ug/ml	ug/ml	ug/ml	ug/ml	ug/ml
NR 8	0.0979	0.4521	3.2087	0.9891	1.0716	0.9131
NR12	0.1313	0.4943	3.5629	1.0563	1.1301	1.0632
NR14	0.1998	0.2524	1.8209	0.8738	0.6617	0.9425
NR15	<0.027	<0.180	2.0572	0.1703	0.3762	<0.030
NR17	<0.027	0.5969	1.3625	0.9013	1.3937	<0.030
NR18	0.0485	0.4884	1.6710	0.6007	0.3860	0.0722
NGB	9.8362	1.1770	30.5711	3.0272	1.2826	7.8127
NGSnow 2-2	<0.027	3.2752	1.5270	0.0468	1.2996	0.0668
NR13	0.3672	0.2758	2.5436	1.0233	0.6829	1.2658
NG Debris	1.7600	1.4497	6.7674	0.9087	0.7223	2.2679
Soil Summit	1.1111	1.2546	13.7271	3.8507	1.4158	116.7123
Hoar Foot Sum	<0.027	0.6725	61.7138	15.3580	2.3735	120.5544
Ice Cave Sum	<0.027	<0.180	0.0555	0.0045	0.0291	0.0758
GB	0.5083	0.4490	2.7741	1.1565	0.6073	1.2610
Paradise Glacier	0.1506	<0.180	0.3515	0.0254	0.0605	0.2813
EGI	12.1551	2.5402	34.3208	3.6030	1.5427	16.8998
NGS cre	0.0441	0.3423	0.1725	0.0231	0.0390	0.1265
NGI	6.2500	0.9010	16.9570	3.1466	0.7482	5.3553
NR16	0.2138	0.2939	2.3566	1.0742	0.6151	1.8737
Para Riv	0.0308	0.6632	2.2339	0.9769	1.8337	<0.030
NGW	<0.027	<0.180	0.3558	0.0471	0.0958	0.1168
TI	0.8646	0.4419	3.8929	1.4893	0.7431	2.1760
E Pond Ice	0.8823	0.3451	4.9442	0.2580	0.2586	4.7417

Analysis on 9/20/2016

Sample ID	P	K	Ca	Mg	S	Al
	ug/ml	ug/ml	ug/ml	ug/ml	ug/ml	ug/ml
NF1	<0.027	0.647	1.293	0.855	1.660	<0.030
NF2	<0.027	0.531	1.290	0.862	1.494	<0.030
T1A	0.951	0.475	4.394	1.771	0.836	3.273
T1B	1.031	0.659	4.155	1.603	0.771	2.631
GB1	0.531	0.465	2.760	1.198	0.637	1.520
GB2	0.632	0.440	3.153	1.342	0.666	2.111
NR14A	0.188	0.334	1.943	0.902	0.670	1.208
NR14B	0.163	0.464	1.891	0.872	0.679	0.983

Analysis on 12/4/12

Sample ID	P	K	Ca	Mg	S	Al
GB-B5	0.1028	0.6337	1.7243	1.2787	1.2761	0.1045
GB-A6	0.0695	0.5660	1.7157	1.2883	1.2662	0.1353

Analysis 10/8/12

Sample ID	P	K	Ca	Mg	S	Al
	ug/ml	ug/ml	ug/ml	ug/ml	ug/ml	ug/ml
NR 8A	0.126	<0.180	3.311	1.071	1.179	1.296
NR 8B	0.075	<0.180	3.359	1.070	1.024	1.315
NR 12A	0.164	<0.180	3.837	1.138	1.186	1.480
NR 13B	0.284	<0.180	2.537	1.154	0.724	1.847
NR 16A	0.195	<0.180	2.273	1.086	0.622	1.765
NR 16B	0.189	0.276	2.469	1.145	0.636	2.344

Analysis on 9/5/2016

Sample ID	B	Cu	Fe	Mn	Mo	Na
	ug/ml	ug/ml	ug/ml	ug/ml	ug/ml	ug/ml
NR 8	0.0144	<0.002	0.3176	0.0219	<0.001	1.9462
NR12	0.0108	<0.002	0.3622	0.0238	<0.001	1.9033
NR14	0.0106	<0.002	0.3170	0.0319	<0.001	1.4258
NR15	0.0043	<0.002	0.0067	<0.001	<0.001	0.8117
NR17	0.0203	<0.002	0.0310	0.0011	<0.001	2.0850
NR18	0.0045	<0.002	0.0048	<0.001	<0.001	1.5615
NGB	0.0014	0.0351	0.3576	0.2904	0.0022	1.2794
NGSnow 2-2	0.0237	0.0029	0.0372	0.0014	<0.001	0.8515
NR13	0.0082	0.0029	0.4628	0.0440	<0.001	1.5514
NG Debris	0.0028	0.0190	0.4719	0.0305	<0.001	0.2938
Soil Summit	0.0089	0.0237	4.5558	0.3204	0.0024	0.3296
Hoar Foot Sum	0.0008	<0.002	0.0451	3.4219	0.0018	0.7419
Ice Cave Sum	0.0010	<0.002	0.0051	<0.001	<0.001	<0.041
GB	0.0059	0.0030	0.3035	0.0858	<0.001	1.3349
Paradise Glacier	<0.000	<0.002	0.0453	0.0015	<0.001	0.0503
EGL	0.0076	0.0789	4.0889	0.4463	0.0015	5.4059
NGS cre	<0.000	<0.002	0.0531	0.0028	<0.001	0.0683
NGI	<0.000	0.0327	1.5005	0.2248	<0.001	0.9733
NR16	0.0048	0.0030	0.5860	0.0522	<0.001	1.5862
Para Riv	0.0161	<0.002	0.0035	<0.001	<0.001	2.9814
NGW	0.0035	<0.002	0.0176	0.0018	0.0016	0.1480
TI	0.0090	0.0069	0.6030	0.1366	<0.001	1.4707
E Pond Ice	0.0029	0.0133	0.3412	0.0160	0.0018	1.4203

Analysis on 9/20/2016

Sample ID	B	Cu	Fe	Mn	Mo	Na
	ug/ml	ug/ml	ug/ml	ug/ml	ug/ml	ug/ml
NF1	0.020	<0.002	0.016	<0.001	<0.001	2.376
NF2	0.022	<0.002	0.029	<0.001	<0.001	2.183
T1A	0.008	0.011	1.114	0.152	<0.001	1.804
T1B	0.008	0.008	0.825	0.145	<0.001	1.650
GB1	0.006	0.005	0.413	0.093	<0.001	1.412
GB2	0.007	0.006	0.689	0.102	<0.001	1.532
NR14A	0.008	0.007	0.434	0.034	<0.001	1.529
NR14B	0.008	<0.002	0.341	0.035	<0.001	1.463

Analysis on 12/4/12

Sample ID

GB-B5	0.0199	<0.002	0.0452	0.0045	<0.001	2.3505
GB-A6	0.0195	<0.002	0.0552	0.0042	<0.001	2.3346

Analysis 10/8/12

Sample ID	B	Cu	Fe	Mn	Mo	Na
	ug/ml	ug/ml	ug/ml	ug/ml	ug/ml	ug/ml
NR 8A	0.010	0.004	0.397	0.022	<0.001	2.185
NR 8B	0.012	0.003	0.405	0.022	<0.001	2.205
NR 12A	0.010	0.003	0.472	0.027	<0.001	2.188
NR 13B	0.011	0.004	0.616	0.052	<0.001	1.813
NR 16A	0.010	0.006	0.540	0.057	<0.001	1.611
NR 16B	0.009	0.007	0.681	0.059	<0.001	1.776

Analysis on 9/5/2016

Sample ID	Zn ug/ml	As ug/ml	Ba ug/ml	Be ug/ml	Cd ug/ml	Co ug/ml
NR 8	0.0036	<0.009	0.0070	<0.000	0.0008	<0.001
NR12	0.0068	<0.009	0.0081	<0.000	0.0005	<0.001
NR14	0.0078	<0.009	0.0085	<0.000	<0.000	<0.001
NR15	0.0031	<0.009	0.0032	<0.000	0.0006	<0.001
NR17	0.0055	<0.009	0.0024	<0.000	0.0005	<0.001
NR18	0.0043	<0.009	0.0021	<0.000	<0.000	<0.001
NGB	0.0195	<0.009	0.0623	0.0007	0.0004	0.0042
NGSnow 2-2	0.0215	<0.009	0.0059	<0.000	<0.000	<0.001
NR13	0.0072	<0.009	0.0108	<0.000	<0.000	0.0011
NG Debris	0.0207	0.0137	0.0225	<0.000	0.0010	<0.001
Soil Summit	0.1285	0.0154	5.8897	0.0058	0.0010	0.0059
Hoar Foot Sum	0.2039	<0.009	6.4989	0.0109	0.0016	0.0367
Ice Cave Sum	0.0030	<0.009	0.0024	<0.000	<0.000	<0.001
GB	0.0049	0.0104	0.0148	<0.000	<0.000	0.0011
Paradise Glacier	0.0047	<0.009	0.0029	<0.000	<0.000	<0.001
EGI	0.0589	<0.009	0.0853	0.0007	0.0004	0.0047
NGS cre	0.0026	<0.009	0.0026	<0.000	<0.000	<0.001
NGI	0.0282	<0.009	0.0502	<0.000	<0.000	0.0035
NR16	0.0052	<0.009	0.0123	<0.000	<0.000	<0.001
Para Riv	0.0021	<0.009	0.0024	<0.000	<0.000	<0.001
NGW	0.0036	<0.009	0.0017	<0.000	<0.000	<0.001
TI	0.0071	<0.009	0.0203	<0.000	<0.000	0.0015
E Pond Ice	0.0089	<0.009	0.0427	<0.000	0.0004	<0.001

Analysis on 9/20/2016

Sample ID	Zn ug/ml	As ug/ml	Ba ug/ml	Be ug/ml	Cd ug/ml	Co ug/ml
NF1	0.010	<0.009	0.005	<0.000	<0.000	<0.001
NF2	0.007	<0.009	0.005	<0.000	0.001	<0.001
T1A	0.098	<0.009	0.033	0.001	<0.000	0.002
T1B	0.048	<0.009	0.026	<0.000	<0.000	0.002
GB1	0.021	<0.009	0.017	0.000	<0.000	0.001
GB2	0.010	<0.009	0.018	<0.000	<0.000	0.002
NR14A	0.011	<0.009	0.013	<0.000	<0.000	<0.001
NR14B	0.010	<0.009	0.011	<0.000	<0.000	<0.001

Analysis on 12/4/12

Sample ID

GB-B5	0.0066	<0.009	0.0345	<0.000	<0.000	<0.001
GB-A6	0.0067	<0.009	0.0019	<0.000	<0.000	<0.001

Analysis 10/8/12

Sample ID	Zn ug/ml
NR 8A	0.029
NR 8B	0.026
NR 12A	0.041
NR 13B	0.071
NR 16A	0.591
NR 16B	0.151

Analysis on 9/5/2016

Sample ID	Cr	Li	Ni	Pb	Sb	Se
	ug/ml	ug/ml	ug/ml	ug/ml	ug/ml	ug/ml
NR 8	<0.001	<0.006	<0.001	<0.004	<0.007	<0.012
NR12	<0.001	<0.006	<0.001	<0.004	<0.007	<0.012
NR14	<0.001	<0.006	<0.001	<0.004	<0.007	<0.012
NR15	<0.001	<0.006	<0.001	<0.004	<0.007	<0.012
NR17	<0.001	<0.006	0.0016	<0.004	<0.007	<0.012
NR18	<0.001	<0.006	<0.001	<0.004	<0.007	<0.012
NGB	0.0020	0.0498	0.0048	<0.004	0.0163	<0.012
NGSnow 2-2	<0.001	<0.006	<0.001	<0.004	<0.007	<0.012
NR13	<0.001	<0.006	0.0014	0.0050	<0.007	<0.012
NG Debris	<0.001	0.0159	<0.001	0.0046	<0.007	<0.012
Soil Summit	0.0060	6.0351	0.0026	<0.004	0.0095	<0.012
Hoar Foot Sum	0.0099	6.6898	0.0221	<0.004	0.0220	<0.012
Ice Cave Sum	<0.001	<0.006	<0.001	<0.004	<0.007	<0.012
GB	<0.001	<0.006	0.0017	<0.004	<0.007	<0.012
Paradise Glacier	<0.001	<0.006	<0.001	<0.004	<0.007	<0.012
EGL	0.0034	0.0669	0.0235	<0.004	0.0152	<0.012
NGS cre	<0.001	<0.006	<0.001	<0.004	<0.007	<0.012
NGI	0.0026	0.0257	0.0123	<0.004	0.0128	<0.012
NR16	<0.001	<0.006	0.0024	<0.004	0.0079	<0.012
Para Riv	<0.001	<0.006	<0.001	<0.004	<0.007	<0.012
NGW	<0.001	<0.006	<0.001	<0.004	<0.007	<0.012
TI	<0.001	0.0098	<0.001	<0.004	<0.007	<0.012
E Pond Ice	<0.001	0.0235	<0.001	<0.004	<0.007	<0.012

Analysis on 9/20/2016

Sample ID	Cr	Li	Ni	Pb	Sb	Se
	ug/ml	ug/ml	ug/ml	ug/ml	ug/ml	ug/ml
NF1	<0.001	<0.006	<0.001	<0.004	<0.007	<0.012
NF2	<0.001	<0.006	<0.001	<0.004	<0.007	<0.012
T1A	<0.001	0.027	0.003	<0.004	0.009	<0.012
T1B	<0.001	0.016	0.002	<0.004	0.008	<0.012
GB1	<0.001	0.009	0.002	<0.004	<0.007	<0.012
GB2	<0.001	0.014	0.001	<0.004	<0.007	<0.012
NR14A	<0.001	<0.006	<0.001	<0.004	<0.007	<0.012
NR14B	<0.001	0.007	<0.001	<0.004	<0.007	<0.012

Analysis on 12/4/12

Sample ID	Cr	Li	Ni	Pb	Sb	Se
GB-B5	<0.001	<0.015	0.0306	<0.001	<0.004	<0.007
GB-A6	<0.001	<0.015	0.0070	<0.001	<0.004	<0.007

Analysis on 9/5/2016

Sample ID	Si	Sr	Tl	V
	ug/ml	ug/ml	ug/ml	ug/ml
NR 8	4.3387	0.0238	0.0074	<0.003
NR12	4.4460	0.0251	0.0038	<0.003
NR14	3.6668	0.0145	<0.003	<0.003
NR15	2.4073	0.0086	<0.003	<0.003
NR17	2.7555	0.0096	<0.003	<0.003
NR18	8.2930	0.0105	0.0037	<0.003
NGB	6.0965	0.1080	<0.003	0.0093
NGSnow 2-2	0.0356	0.0072	<0.003	<0.003
NR13	4.0849	0.0175	<0.003	<0.003
NG Debris	0.3718	0.0248	<0.003	<0.003
Soil Summit	3.9101	0.3087	0.0049	0.0206
Hoar Foot Sum	13.7407	1.0783	<0.003	0.0049
Ice Cave Sum	0.0045	<0.000	<0.003	<0.003
GB	3.3601	0.0178	<0.003	<0.003
Paradise Glacier	0.1551	0.0010	<0.003	<0.003
EGL	12.9076	0.1999	<0.003	0.0440
NGS cre	0.0770	0.0009	0.0035	<0.003
NGI	3.5210	0.0591	<0.003	0.0136
NR16	4.7465	0.0203	<0.003	<0.003
Para Riv	5.0047	0.0137	<0.003	<0.003
NGW	0.3353	0.0018	<0.003	<0.003
TI	3.8939	0.0250	<0.003	<0.003
E Pond Ice	2.4061	0.0444	<0.003	<0.003

Analysis on 9/20/2016

Sample ID	Si	Sr	Tl	V
	ug/ml	ug/ml	ug/ml	ug/ml
NF1	2.865	0.009	<0.003	<0.003
NF2	2.835	0.009	<0.003	<0.003
T1A	5.355	0.033	<0.003	<0.003
T1B	4.660	0.028	<0.003	<0.003
GB1	3.822	0.019	<0.003	<0.003
GB2	4.432	0.023	<0.003	<0.003
NR14A	4.176	0.016	<0.003	<0.003
NR14B	3.908	0.015	<0.003	<0.003

Analysis on 12/4/12

Sample ID	Si	Sr	Tl	V
GB-B5	<0.012	4.2158	0.0116	<0.003
GB-A6	<0.012	4.3138	0.0105	<0.003